AD-A214 168

REPORT DOCUMENTATION PAGE

1a. REPORT SECURITY CLASSIFICATION UNCLASSIFIED	1b. RESTRICTIVE MARKINGS

2a. SECURITY CLASSIFICATION AUTHORITY	3. DISTRIBUTION / AVAILABILITY OF REPORT
2b. DECLASSIFICATION / DOWNGRADING SCHEDULE	Approved for public release; distribution unlimited.

4. PERFORMING ORGANIZATION REPORT NUMBER(S) N00014-85-C-0141-AR9	5. MONITORING ORGANIZATION REPORT NUMBER(S)

6a. NAME OF PERFORMING ORGANIZATION Washington State University	6b. OFFICE SYMBOL (If applicable)	7a. NAME OF MONITORING ORGANIZATION Office of Naval Research

6c. ADDRESS (City, State, and ZIP Code) Department of Physics Washington State University Pullman, WA 99164-2814	7b. ADDRESS (City, State, and ZIP Code) Physics Division, Code 1112 Arlington, VA 22217-5000

8a. NAME OF FUNDING / SPONSORING ORGANIZATION	8b. OFFICE SYMBOL (if applicable)	9. PROCUREMENT INSTRUMENT IDENTIFICATION NUMBER N00014-85-C-0141

8c. ADDRESS (City, State, and ZIP Code)	10. SOURCE OF FUNDING NUMBERS			
	PROGRAM ELEMENT NO.	PROJECT NO.	TASK NO.	WORK UNIT ACCESSION NO
	61153N	4126934		

11. TITLE (Include Security Classification)
Research on Acoustical Scattering, Diffraction Catastrophes, Optics of Bubbles, Acoustical Phase Conjugation, and Wake of an Oscillating Circular Cylinder

12. PERSONAL AUTHOR(S)
Marston, P. L.

13a. TYPE OF REPORT Annual Summary	13b. TIME COVERED FROM 881016 TO 891015	14. DATE OF REPORT (Year, Month, Day) 891031	15. PAGE COUNT 56

16. SUPPLEMENTARY NOTATION The telephone number for the Principal Investigator, P. L. Marston, is (509)335-5343. Researchers include: S.G. Kargl, C.E. Dean, H.J. Simpson, J.M. Winey, and J.R. Filler.

19 ABSTRACT (Continue on reverse if necessary and identify by block number)

The research summarized concerns several aspects of the propagation and scattering of acoustical and optical waves. The topics discussed fall under the following five categories:

A. Project to extend GTD (ray methods) to guided waves on smooth elastic objects in water as tested by synthesis of the forward and backward scattering amplitudes of a spherical shell and the total scattering cross section, thickness resonance and curvature correction to the specular contribution to backscattering from a shell; and a numerical test of the product expansion of the S function for scattering.

20. DISTRIBUTION / AVAILABILITY OF ABSTRACT ☒ UNCLASSIFIED/UNLIMITED ☐ SAME AS RPT ☐ DTIC USERS	21 ABSTRACT SECURITY CLASSIFICATION UNCLASSIFIED
22a. NAME OF RESPONSIBLE INDIVIDUAL L. E. Hargrove, ONR Physics Division	22b. TELEPHONE (Include Area Code) (209) 696-4221	22c. OFFICE SYMBOL ONR Code 1112

DD Form 1473, JUN 86   Previous editions are obsolete.   SECURITY CLASSIFICATION OF THIS PAGE

UNCLASSIFIED

89 11 06 172

19. ABSTRACT (Continued)

B. Acoustical and optical caustics and associated wavefields: opening rate in the transverse cusp in light scattered from oblate water drops; scaling laws and wavefront shape for light backscattered from oblate drops; observations of acoustical and optical transverse cusps produced by reflection; and miscellaneous applications.

C. Physical optics of bubbles in water: an asymptotic series for critical angle scattering useful for determining bubble sizes.

D. Acoustic phase conjugation and aspects of wavefront reversal: the present status of experiments on three-wave mixing in a layer of microbubbles in water; and preliminary aspects of an experiment with phase conjugation of ripples on layer of water.

E. Response of the wake of a circular cylinder to forced torsional oscillations: waves on shear layers and effects on primary and secondary vortices.

1

DEPARTMENT OF PHYSICS

WASHINGTON STATE UNIVERSITY

PULLMAN, WA   99164-2814

ANNUAL SUMMARY REPORT

OCTOBER, 1989

Title:

Research on Acoustical Scattering, Diffraction Catastrophes, Optics of

Bubbles, Acoustical Phase Conjugation, and Wake of an Oscillating

Circular Cylinder

by

Philip L. Marston

Prepared for:

OFFICE OF NAVAL RESEARCH

PHYSICS DIVISION-CODE 1112

CONTRACT NO. N00014-85-C-0141

Accesion For

NTIS CRA&I

DTIC TAB

Unannounced

Justification

By

Distribution /

Availability Codes

Dist	Avail and/or Special

A-1

ABSTRACT

The research summarized concerns several aspects of the propagation and scattering of acoustical and optical waves and waves on a hydrodynamic shear layer. The topics discussed fall under the following five categories:

A.   Project to extend GTD (ray methods) to guided waves on smooth elastic objects in water as tested by synthesis of the forward and backward scattering amplitudes of a spherical shell and the total scattering cross section; thickness resonance and curvature correction to the specular contribution to backscattering from a shell; and a numerical test of the product expansion of the S function for scattering.

B.   Acoustical and optical caustics and associated wavefields: opening rate in the transverse cusp in light scattered from oblate water drops; scaling laws and wavefront shape for light backscattered from oblate drops; observations of acoustical and optical transverse cusps produced by reflection; and miscellaneous applications.

C.   Physical optics of bubbles in water: an asymptotic series for critical angle scattering useful for determining bubble sizes.

D.   Acoustic phase conjugation and aspects of wavefront reversal: the present status of experiments on three-wave mixing in a layer of microbubbles in water; and preliminary aspects of an experiment with phase conjugation of ripples on layer of water.

E.   Response of the wake of a circular cylinder to forced torsional oscillations: waves on shear layers and effects on primary and secondary vortices.

TABLE OF CONTENTS

I. SCATTERING OF SOUND FROM ELASTIC OBJECTS IN WATER

A. Project to Extend GTD (Ray Methods) to Guided Waves on Smooth Elastic Objects

The extension of the geometrical theory of diffraction (GTD) to backscattering from elastic objects in water should allow complicated scattering problems to be partitioned into geometry and the determination of local guided-wave/acoustic-field interactions from continuum mechanics. It gives a simple and quantitative understanding of the scattering process which could be useful both for inverse problems and for prediction of how changes in an object will affect the scattering. Heuristic support for the basic ideas were put forth by Soviet researchers[1] and in a rigorous way (for the special case of a solid elastic sphere) by Williams and Marston.[2,3] In previous Annual Reports[4,5] the development and initial testing[6] are summarized for a simple approximation of the relevant complex coupling coefficient G_l for the lth class of surface elastic wave (SEW) for the case of spheres and circular cylinders. Relevant measurements of backscattering of short tone bursts from one empty spherical shell which support the approximations were published.[7] The majority of the new research (summarized below) concerns computational tests of this method of approximating scattering amplitudes based on comparison with exact calculations for hollow elastic shells. For a more detailed summary of the method (and some of the relevant equations) see the INTRODUCTION to the manuscript[8] reproduced here in Appendix A.

The present ray method for a quantitative description of SEW by Marston has a limitation relevant to the scattering from thin shells. The method as formulated assumes that the phase velocity c_l (along the outer surface) of the Lamb waves of interest exceeds the phase velocity in water c. This need not be the case for a flexural wave on a thin shell at sufficiently low frequencies. This limitation is not fundamental to calculations of amplitudes with a ray representation according to a recent formulation by Felsen et al.[9]

While the formulation by Felsen et al. is more general than that by Marston,[6-8] with the support of the present contract there has been several numerical verifications of Marston's formulation based on comparisons with exact computations. Recent and novel examples are discussed here. Other relevant formulations include ray treatments of propagation on thin-walled elastic shells[10,11] and Marston's simple approximation[12] of the curvature correction for c_l.

There has also been progress in recognizing what physical processes may be relevant to the resolution of unresolved issues in ray formulations. New experiments on scattering from *elastic* objects were not carried out due to plans to substantially improve the experimental facility and because of other uses of the existing facility for contract research on this contract.

In addition to the research on scattering from elastic objects summarized below, Marston has made novel corrections and applications during the formulation of a review chapter for *Physical Acoustics* (Academic Press). See Sec. II E.

B. Synthesis of Forward Scattering Amplitudes from a Spherical Shell and the Total Scattering Cross Section

Kargl and Marston[13] have verified that the ray formulation is applicable to forward scattering and the total cross section by comparison with exact computations for a shell of radius a. Figure 1 shows the ray diagram and the mechanisms are summarized in the captions. The total acoustic pressure p_t, form function $f(\theta)$, and total (extinction) cross section σ_e are related by

$$p_t = p_{inc} \left[e^{ikz} + (a/2r)f(\theta)e^{ikr} \right], \qquad (\sigma_t /\pi a^2) = (2/x)Im\left\{ f(\theta = 0) \right\} \qquad (1,2)$$

where Eq. (2) is a statement of the optical theorem[14], x = ka, θ denotes the scattering angle. The ray picture, Fig. 1, yields the synthesis

Fig. 1 Acoustic ray diagram for Lamb wave contributions to the forward scattering amplitude for Lamb waves having $c_l > c$. The outer radius of the shell is a and the inner radius is b. The incident acoustic plane wave launches a Lamb wave in the vicinity of point B. The Lamb wave propagates along the shell and radiates in the forward direction at point B'. The points B and B' are determined by $\theta_l = \arcsin(c/c_l)$. The qualitative features of the ray diagram are made quantitative through an expression for f_l given in Ref. 13. The GTD also contains a contribution due to diffraction about the shell. That includes contributions due to rays which touch the shell near E at the edge.

Figure 2

The vertical axis is labelled $\dfrac{\sigma_t}{\pi a^2}$ with values 0.0, 0.5, 1.0, 1.5, 2.0, 2.5, 3.0, 3.5, 4.0, 4.5. The horizontal axis is labelled ka with values 0, 5, 10, 15, 20, 25.

$$f(\theta = 0) \approx f_{FD} + \sum_l f_l, \qquad l = \text{Lamb wave type}, \qquad (3)$$

where f_l for the elastic wave contributions has a simple ray representation and f_{FD} is the ordinary forward diffraction contribution . For the purposes of this summary we need only note that f_l is linearly proportional to the coupling coefficient G_l and that to evaluate G_l, Marston's approximation is used[6,8]

$$G_l \approx 8\pi\beta_l \; c/c_l \qquad (4)$$

Figure 2 compares the resulting synthesis (dashed curve) with the results of exact calculations passed on the partial wave series (solid curve) for an empty stainless steel sphere in water.[13,15] The ratio of inner to outer radius b/a is 0.838 and the material properties are as listed in Ref. 7. This synthesis (and the one in Fig. 3) were terminated for $ka \leq 7$ since for t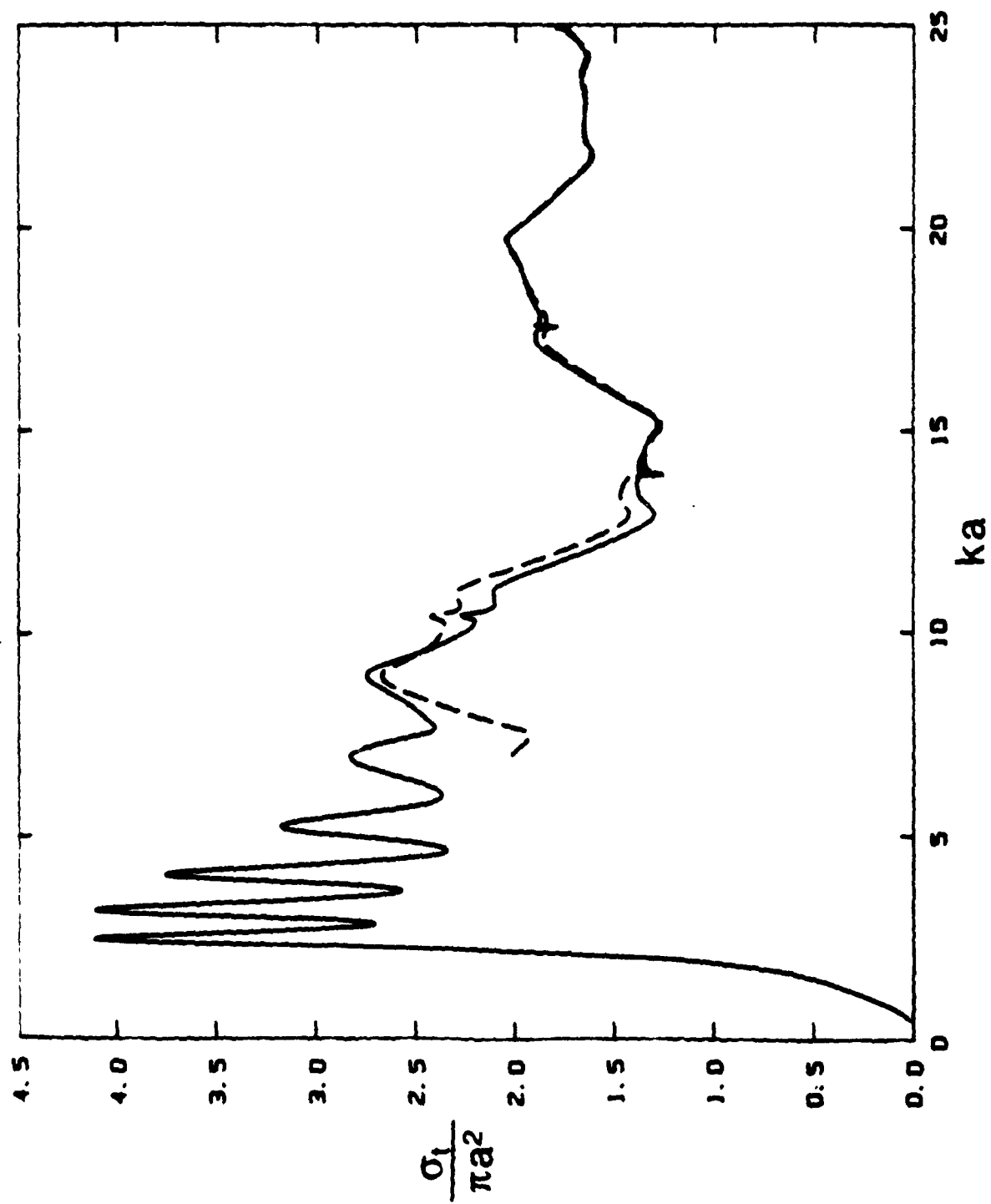hat region the flexural Lamb wave becomes subsonic. Only the $l = a_0$ and s_0 waves are included in the sum over l in Eq. (13) and the agreement in Fig. 2, while not perfect confirms the utility of the approximations. The agreement with the exact result is similar for ka up through 100 when the number of l is increased as the cut off frequency of each mode is crossed.

This model also gives a simple geometrical picture and approximate expressions by which the quai-periodic structures in σ_t may be understood.[13,15] The structure is also associated with forward glory scattering.

C. Synthesis of Backscattering from a Spherical Shell.

The Relevant approximations in this case are given by Eqs. (1), (10), (11) and (13) of Appendix A where the physical content is also discussed. The ray representation is as shown in Fig. 1 of Appendix A. Figure 4 of Appendix A, which is reproduced in larger size here as Fig. 3, compares the synthesis of |f| (dashed curve) with the exact computation
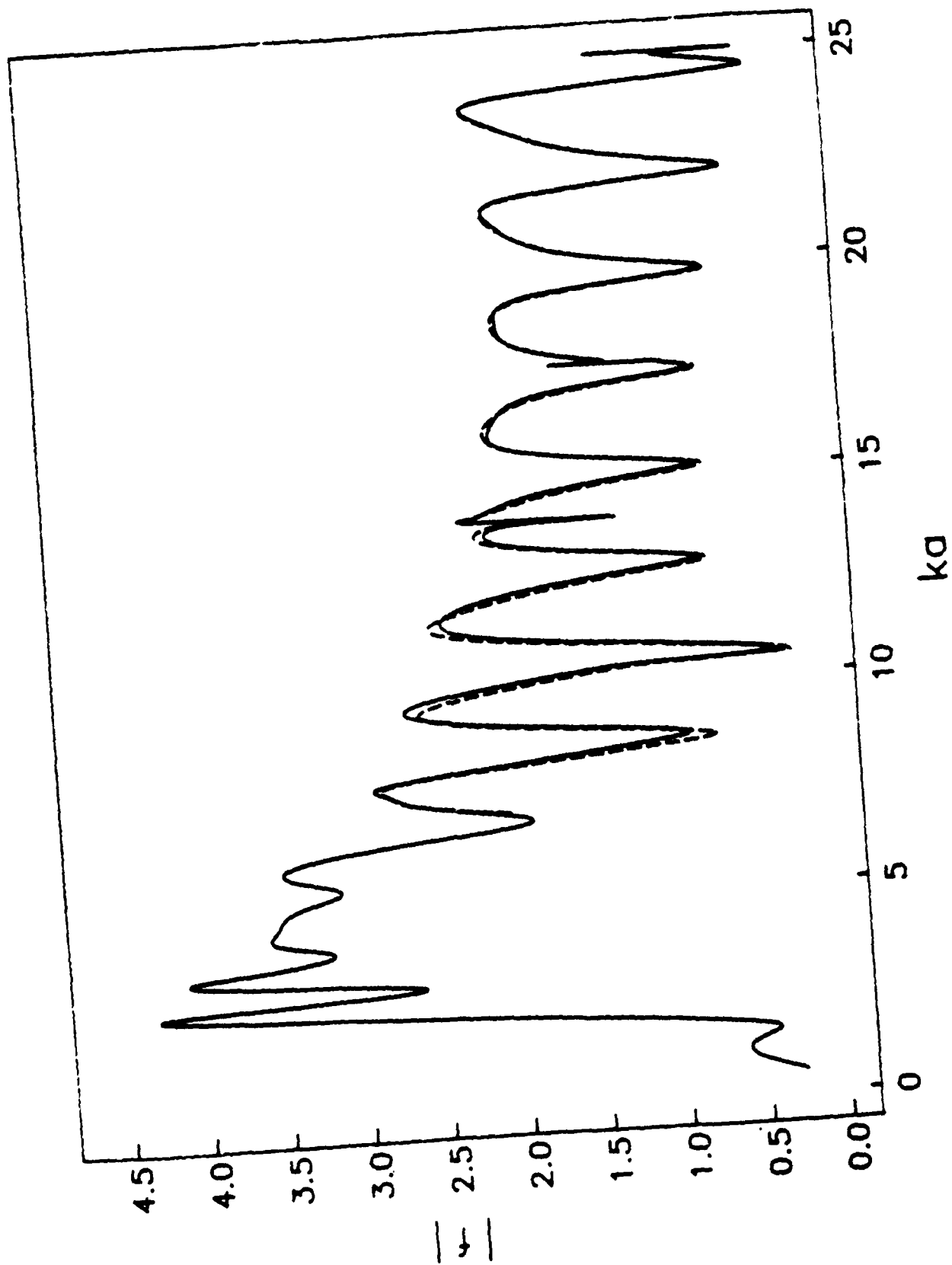
Figure 3

(solid curve). The agreement is good for $ka \geq 7$ through $ka = 100$, with additional l included as each cut off frequency is crossed, except for the region roughly between $ka \approx 70$ and $ka \approx 80$. Two phenomena occur in this frequency region which degrade the usefulness of the approximation:

(i) Based on root locations of $D_\nu(ka)$ in the complex ν plane, the $l = s_1$ cut off is close to $ka = 70$ so that wave type contributes for $ka \geq 70$;

(ii) there is a thickness resonance of the shell in this region due to the axial reverberations of bulk longitudinal waves.[7] See Sec. D below.

In summary: except in the region where (i) and (ii) are relevant and where $c_l \leq c$, the synthesis gives good agreement with the exact calculation. Hence a simple ray representation can give a useful quantitative backscattering amplitude for a shell.[16,17]

D. Thickness Resonance and Curvature Corrections to the Specular Contribution to Backscattering from a Shell

Kargl[17] has made significant progress towards eliminating the errors introduced by the phenomena (ii) noted above. As is evident from Eqs. (10) and (11) of Appendix A and the associated discussion, the approximation of the specular contribution f_S uses the complex reflection coefficient $\mathcal{R}$ of a flat plate and neglects the curvature correction f_{Scc}. The correction accounts for the fact that the inner radius b differs from a so that the strength of reverberations is reduced by additional spreading factors. Figure 4 shows a simplified ray diagram for the problem of interest for which a bulk longitudinal wave is excited in the material having a velocity $c_L > c$ where c is the phase velocity in the water external to the shell. The rays arising from the internal reflections spread at a different rate from that of the specular reflection from the outer surface. For an elastic shell and incident ray displaced from the axis (as drawn in Fig. 4) there will be some mode conversion to shear waves at each vertex. Mode conversion vanishes for rays which are exactly backscattered since they are normally incident on each interface. The discussion which follows neglects
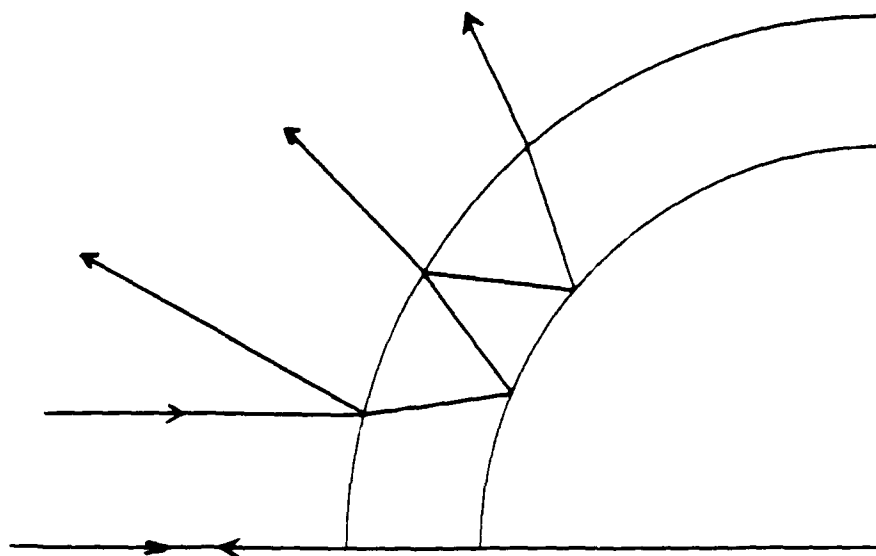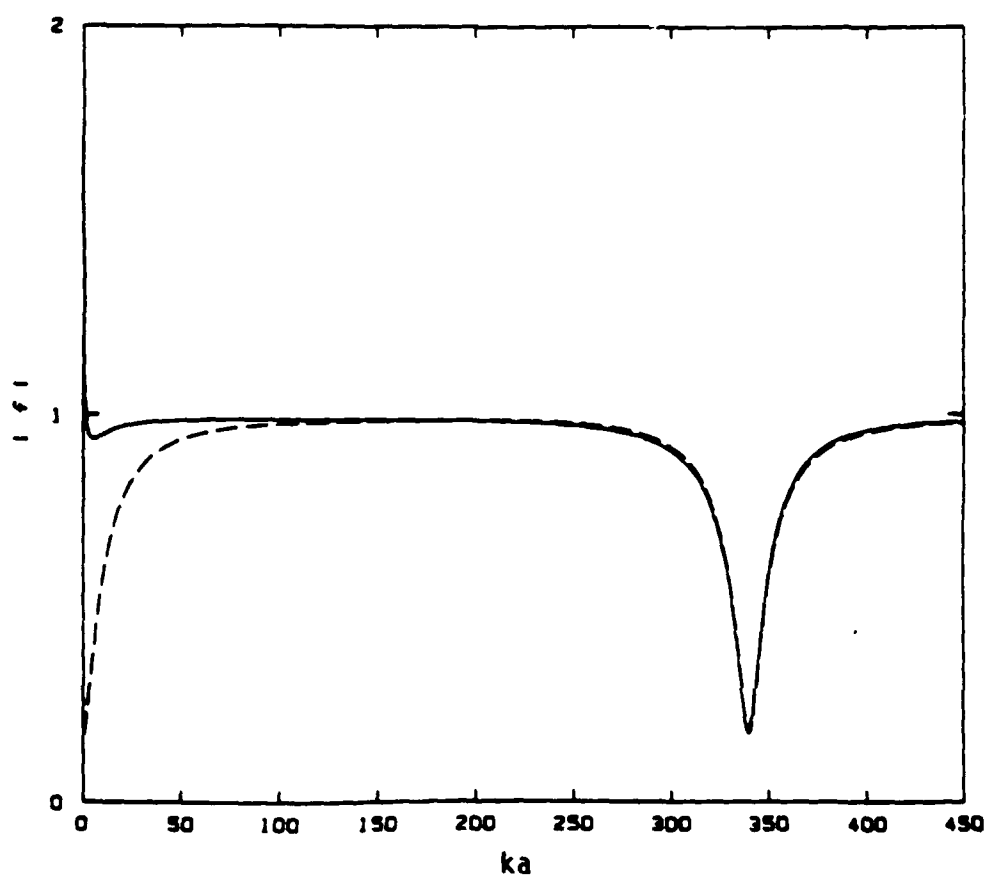
Figure 4

ka

Figure 5

such mode conversion and is directly applicable to the idealized case of an empty fluid shell surrounded by water. It is verified by comparison with exact computation for backscattering from such an idealized shell for which the shear wave speed $c_s = 0$ since the shell material is unable to support shear stress for the case of a fluid shell.

For frequencies such that multiple reverberations are reflected backward from a flat plate such that the successive contributions are in phase with each other, it is conventional to describe the condition as a[18] "longitudinal resonance". The same condition can be present for a spherical layer, though it is presently uncertain as to how such a resonance manifests itself in the analytic properties of the scattering amplitude described in Ref. 6 and here in Sec. I E. For the usual case where $\rho_E c_L > \rho c$, where ρ_E and ρ are the densities of the layer and water, respectively, the lowest resonance condition is that one-half a wavelength of the longitudinal wave fits across the layer. Hence for a spherical shell of thickness $h = a - b$, the lowest resonance is at a frequency $\omega/2\pi = c_L/2h$ corresponding to[7]

$$(ka)_L = \pi c_L/c(1 - b/a). \tag{5}$$

In Kargl's ray analysis, the curvature correction f_{Scc} in Eq. (10) of Appendix A [call it Eq. (A10)] is significant for ka close to $(ka)_L$. The following form is obtained[17]

$$f_{Scc} = \frac{(1 - r^2)}{r} [\exp(-i2ka)] \sum_{n=1}^{\infty} \frac{nBr^n \exp(in\alpha)}{1 + nB} \tag{6}$$

where $\alpha = 2khc/c_L$ and the constant B is a function of b/a and c/c_L. The improved approximation for $|f_S|$ from Eq. (A10) was compared with exact $|f|$ for backscattering from empty fluid shells. Figure 5 shows the comparison for the form function for backscattering from an empty "fluid aluminum" shell in water with b/a = 0.96 and the parameters are $c_L = 6.42$ km/s, $\rho_E = 2.7$ g/cm^3, c = 1.4825 km/s, and $\rho = 1.0$ g/cm^3. The solid curve is the exact calculation based on the partial-wave series where the velocity of the shear wave in the shell material vanishes. The dashed curve is the curvature corrected specular reflection calculated as described above. If the curvature correction f_{Scc} is omitted the approximate

result from Eq. (A10) becomes $|f_S| = 1$ which is clear disagreement with the exact curve which shows a dip near the lowest thickness resonance at $(ka)_L = 340.1$. Clearly f_{Scc} is significant for ka close to $(ka)_L$ and it is will approximated by the geometrical model, Eq. (6).

The implications for the modeling of backscattering from elastic shells (for which the shear velocity does not vanish) are also being explored.

E. Product Expansion of the S Function for Scattering from Elastic Spheres Having Multiple Resonances

In related work, the implicit assumptions of formal resonance scattering theory[19] (RST) have been corrected and clarified. The summary below, while including some of the discussion from the previous *Annual Report*[5], summarizes and displays results of *novel numerical tests* which verify for the first time the corrections to resonance scattering theory. Associated with the scattering phase shift δ_n of the nth partial wave for a sphere of radius a is the function $S_n(x) = \exp[2i\delta_n]$ where $x = ka$. The connection of the S function to the partial-wave form function f_n for backscattering from a sphere is through the relation[19]

$$f_n = \left[(S_n - 1)/2i\right] g_n , \qquad g_n = 2(-1)^n(2n+1)/x, \qquad (7,8)$$

where g_n is introduced for convenience. A theorem from *classical* scattering theory[20] was applied by Marston to obtain the following *product expansion* which appears to be important and novel for acoustics

$$S_n = S_n^{(b)} S_n^{(e)} , \quad S_n^{(b)} = \pm\, e^{-2ix} \prod_j \frac{(iL_{nj} - x)}{(iL_{nj} + x)} , \quad S_n^{(e)} = \prod_l \frac{(x_{nl}^* - x)(x_{nl} + x)}{(x_{nl}^* + x)(x_{nl} - x)} , \quad (9a,b,c)$$

where the $x_{nl} \equiv X_{nl} - i(\Gamma_{nl}/2)$ lie in the fourth quadrant and $L_{nj} > 0$. Unlike a *sum* expansion (stated in some acoustic RST literature[19]) S_n remains manifestly unitary even for

multiple resonances l since $\left|S_n^{(b)}\right| = \left|S_n^{(e)}\right| = 1$. This S_n may be used to split off the elastic and background contributions to $f_n^{(e)}$ and $f_n^{(b)}$ respectively, to f_n as follows

$$f_n = f_n^{(b)} + f_n^{(e)}, \quad f_n^{(b)} = \left[(S_n^{(b)} - 1)/2i\right]g_n, \quad f_n^{(e)} = \left[(S_n^{(e)} - 1)/2i\right]g_n S_n^{(b)} \qquad (10a,b,c)$$

where $S_n^{(b)}$ and $S_n^{(e)}$ are background and elastic factors to S_n from Eq. (9). In partial analogy with the single resonance case of RST the following result was derived for the case of only two resonances (labeled $l = 1$ and 2)

$$f_n^{(e)} \approx f_{n1} + f_{n2} + f_n^{(int)} + f_n^{(L)}, \qquad (11)$$

where it is assumed that $x + X_{nl} \gg \Gamma_{nl}$. The f_{nl} have a Breit-Wigner form

$$f_{nl} = S_n^{(b)} g_n \Gamma_{nl} \left[X_{nl} - x - (i/2)\Gamma_{nl}\right]^{-1} \qquad (12)$$

The implicit assumptions of RST are that S_n has the product form, Eq. (9), and not the sum expansion usually written.[19] Furthermore, the *interaction term* $f_n^{(int)}$ and the contribution $f_n^{(L)}$ from poles in the left-half of the complex ka plane are neglected when $f_n^{(e)}$ is written as a sum of Breit-Wigner terms as is usually done in RST.

Marston's analysis yields the following approximations for the interaction and left-pole contributions in Eq. (11):

$$f_n^{(int)} \approx (i/2)g_n S_n^{(b)} \prod_{l = 1,2} \left(\frac{\Gamma_{nl}}{x - X_{nl} + (i/2)\Gamma_{nl}}\right), \qquad (13)$$

$$f_n^{(L)} = -g_n S_n^{(b)} \left(\sum_{l = 1,2} \frac{\Gamma_{nl}/2}{x + X_{nl}}\right) \prod_{l = 1,2} \left(\frac{x - X_{nl} - (i/2)\Gamma_{nl}}{x - X_{nl} + (i/2)\Gamma_{nl}}\right). \qquad (14)$$

To test these results numerically the following normalized scattering amplitudes were calculated: the exact amplitude $f_n^{(e)}/g_n S_n^{(b)} = (S_n^{(e)} - 1)/2i$ from Eq. (10c), and the corresponding approximate result from Eqs. (11) - (14). To evaluate these, it was necessary to select the resonance frequency x_{nl} and damping Γ_{nl} parameters so as to evaluate either Eq. (9c) or Eqs. (12) - (14) in the exact or approximate cases respectively.
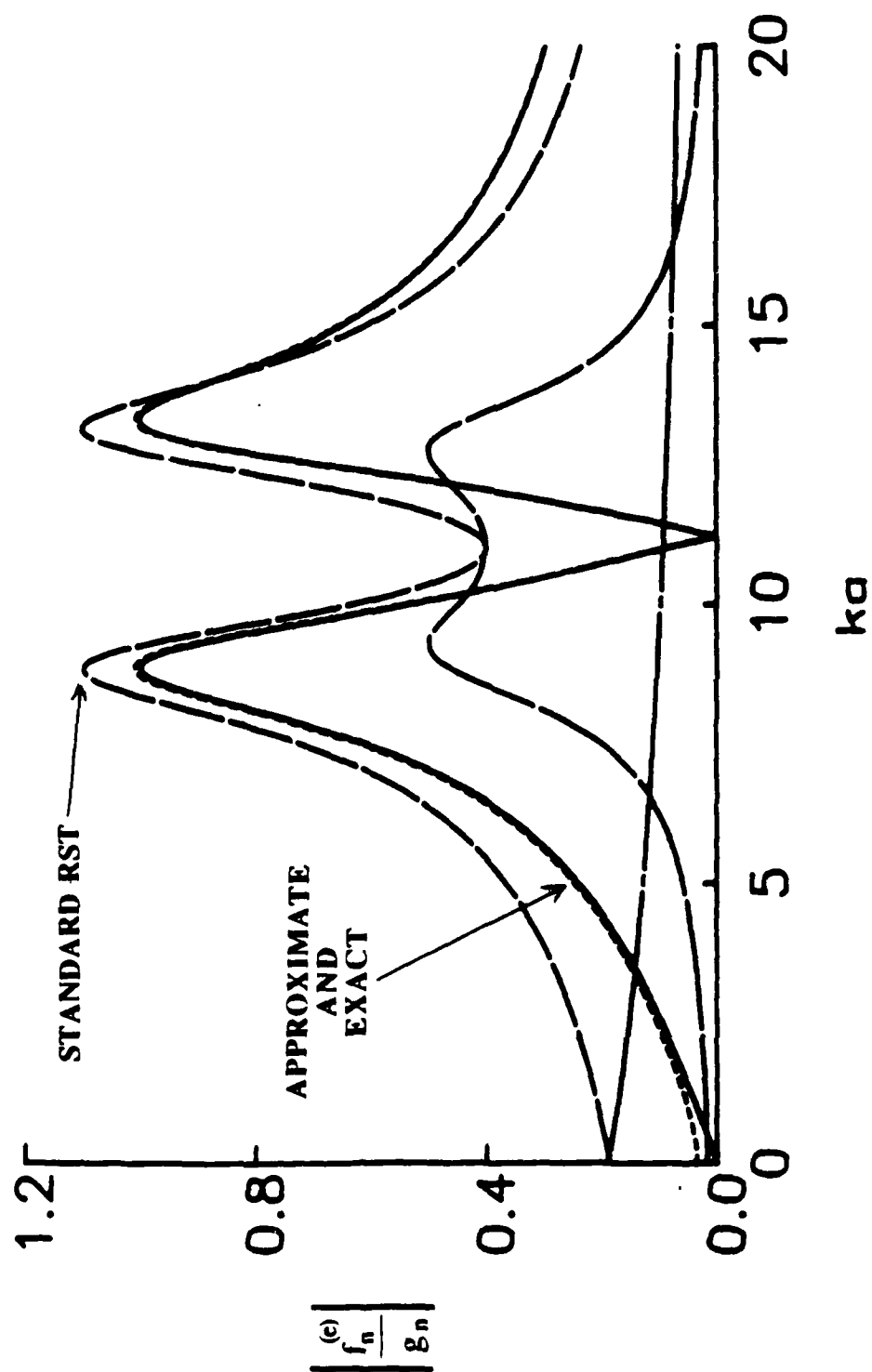
Figure 6

Figure 6 shows a representative comparison for which $X_{n1} = 9$, $X_{n2} = 13$ and $\Gamma_{n1} = \Gamma_{n2} = 2$ where the modulus of the aforementioned quantities are plotted. The solid curve is the exact result $|(S_n^{(e)} - 1)/2i|$ while superposed (and almost indistinguishable from it) is a short dashed curve giving the aforementioned approximate result. In "standard" RST[19], the terms $f_n^{(int)}$ and $f_n^{(L)}$ are omitted in Eq (11) which yields the intermediate length dashed curve which fails to describe the null between resonances present in the exact result. Also shown in Fig. 6 are the normalized magnitudes of the interaction and left-pole terms considered alone, the long-dashed and alternate dashed terms respectively.

This numerical test, and similar results with other resonance parameters confirm the analysis leading to Eqs. (12) - (14). They also suggest that the interaction term may be quite significant between resonances and that the left-pole contribution is important at low ka.

The tests described above do not directly depend on the nature of the background contribution. The product expansion over index j in Eq. (9b), manifestly corresponds to poles (or generalized resonances) for which there is no restoring force but only damping. (These poles lie on the imaginary axis at $x = -iL_{nj}$.) The physical significance of such a pole is illustrated by considering the $n = 1$ or dipole partial-wave. The L_{1j} pole(s) account for the translational motion of a movable elastic sphere.

II. ACOUSTICAL AND OPTICAL CAUSTICS AND ASSOCIATED WAVEFIELDS (DIFFRACTION CATASTROPHES)

A. Project to Explore novel acoustical and Optical Diffraction Catastrophes or Other Wavefields Near Caustics

In previous research we described examples of acoustical and optical diffraction catastrophes in certain reflection and scattering problems.[4,5] Such catastrophes decorate the caustics of geometrical optics where the amplitudes of the wavefields tend to be large when the wavelength is short. Three recent accomplishments are described below.

B. Opening Rate in the Transverse Cusp in Light Scattered from Oblate Water Drops

This research is concerned with calculating properties of a far field transverse cusp caustic Marston previously observed in light scattered from acoustically levitated horizontally-illuminated oblate drops of water.[21-23] It follows from the analysis given in Ref. 23 that a far field cusp caustic has the form

$$d_\infty (U - U_{cp})^3 = V^2. \tag{15}$$

where U and V are local horizontal and vertical scattering angles in radians, U_{cp} specifies the cusp point location, and d_∞ is the angular opening rate (in radians^{-1}) of the cusp caustic. As part of his Ph.D. Thesis project, C. Dean calculated d_∞ for the cusp associated with the once internally reflected ray from an oblate water drop.[24,25] The calculation gave d_∞ as a function of the drop oblateness q = D/H where D is the drop's horizontal diameter and H the drop length (or vertical thickness). The analysis is supported by measurements obtained from photographs of scattering patterns.

The method and results of the analysis are summarized below. The outgoing wavefront leading to the transverse cusp caustic was previously shown to be of the form[23]

$$W(x,y) = -(a_1 x^2 + a_2 y^2 x + a_3 y^2), \tag{16}$$

where x and y are horizontal and vertical cartesian coordinates. It follows as a special case of the analysis given in Ref. 23 that $d_\infty = 4a_2/27a_1^2$. Hence the problem of determining d_∞ reduces to the calculation of this function of the wavefront shape parameters a_1 and a_2 for the wavefront leaving the drop. Dean accomplished this by applying a method of wavefront tracing in which the principal curvatures of the wavefront are calculated at successive positions in the drop. (The technique, also known as generalized ray tracing, was developed for optical instrument design[26] but was applied to other aspects of scattering from drops previously by Marston.[4,25,27]) The resulting prediction for d_∞ is shown in
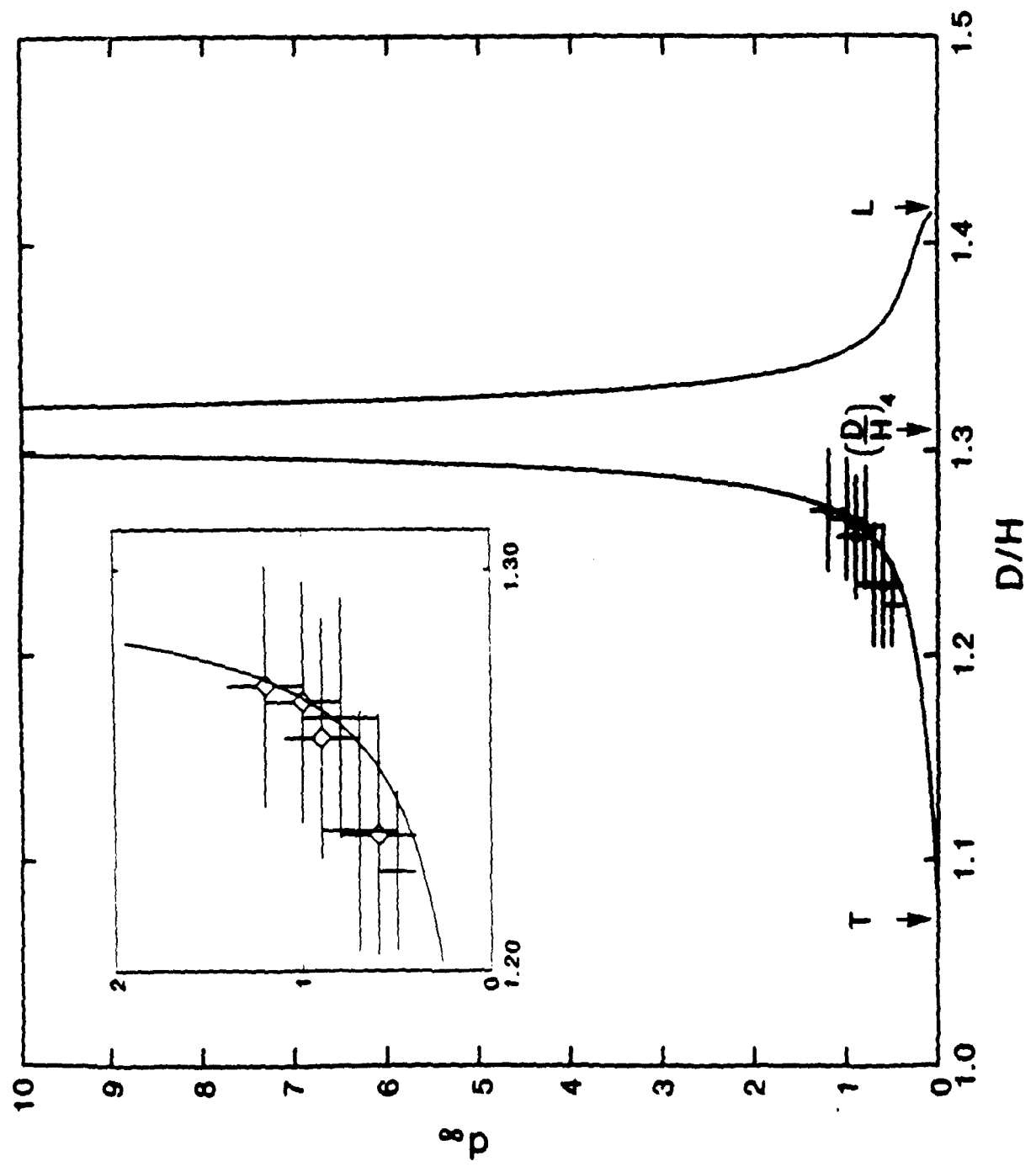
Figure 7

Fig. 7 for an oblate spheroidal drop of oblateness q and refractive index N = 1.332. The data and error bars were obtained by measuring the opening rate from photographs of the scattering pattern like those shown in Ref. 21-23. The crosses correspond to cases where q = D/H was measured from photographs of the drop. For the open diamonds, D/H was inferred from a measurement of the cusp point location and using the analysis given in Ref. 22. The inset shows the region of experimental data on an enlarged scale. The measurements support the analysis though the measurement uncertainties (error bars) are larger than would be otherwise desired in part because of complexities of the photographic and levitation techniques.

A brief discussion of the qualitative features of the curve in Fig. 7 is merited to facilitate a discussion of related work in Sec. II C. It was previously shown[22,28] that when q = (D/H)$_4$ $\approx$ 1.311, the scattering pattern ins that of a hyperbolic umbilic focal section in which the caustics are straight lines. Consequently, it is to be expected that d$_\infty$ diverges as q approaches (D/H)$_4$ as shown in Fig. 7. Furthermore, from the analysis of Nye,[28] it is to be expected that as q approaches the lips event at

$$q_{L1} = (D/H)_{L1} = \left[N/(2N - 2)\right]^{1/2} \approx 1.416, \tag{17}$$

the opening rate d$_\infty$ vanishes. This corresponds to point L in Fig. 7. Dean's numerical results[28] show that d$_\infty$ near q$_{L1}$ scales as

$$d_\infty \approx B \, (q_{L1} - q)^{1/2}, \tag{18}$$

where B is a constant. The analysis also shows that d vanishes as q approaches the transition event[22] labeled T in Fig. 7.

C. Lips Caustics in Light Backscattered from Oblate Drops

Catastrophe theory allows the caustics leaving two cusp points to join smoothly. The resulting bounded caustics have the appearance of a pair of lips as shown in Fig. 8.

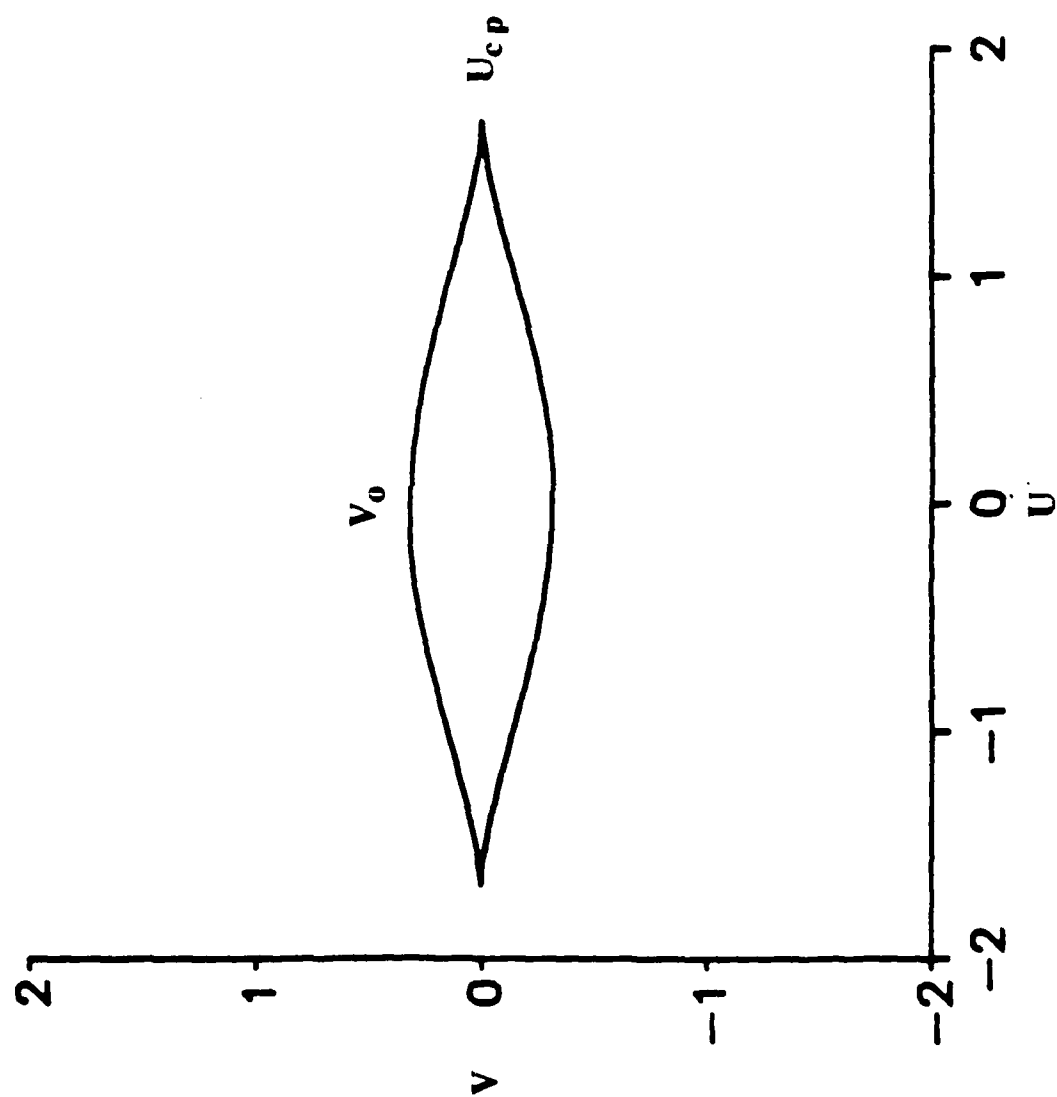## LIPS CAUSTIC

V_o

U_{cp}

Figure 8

This curve was calculated as summarized below, by a graduate student, Harry Simpson. As noted in conjunction with Eq. (17) above, Nye predicted[28] that lips caustics occur in the backscattering from horizontally illuminated sufficiently oblate drops. The "lips" should close and disappear as the aspect ratio $q = D/H$ reaches q_{L1} of Eq. (17). In previous previous research, Simpson obtained photographic evidence of this prediction.[5,27,29]

In research during the past year, Simpson has improved the acoustic levitator and has obtained higher quality photographs of lips caustics than those previously obtained.[5,27,29] Simpson has also made significant progress on the theory of lips caustic and the lips event, the quantitative results of which are summarized below. For q somewhat smaller than q_{L1}, a lips caustic as shown in Fig. 8 should be produced. The associated outgoing wavefront leaving the drop was argued from symmetry to have the local shape

$$W = -(a_1 x^2 + a_2 y^2 x^2 + a_3 y^2 + a_4 y^4), \tag{19}$$

where x and y are horizontal and vertical cartesian coordinates with $x = y = 0$ along the backward axis. Figure 8 is the farfield caustic from the W in Eq. (19) calculated for an appropriate choice of wavefront shape parameters a_j. As q approaches q_{L1}, a_3 must vanish. Using results Ref. 22 for the cusp point location at the edge of the lips and the form of Eq. (19) the following new scaling laws were derived which are applicable for q close to q_{L1}:

$$U_{cp} = A \, (q_{L1} - q)^{1/2}, \qquad V_o = C(q_{L1} - q)^{3/2}, \tag{20a,b}$$

where A and C are constants. Here U_{cp} is the cusp point angle relative to the backward axis and V_o is the angle relative to the backward axis to the top of the lips (i.e. where the smooth caustic crosses the V axis at $U = 0$). There are marked in Fig. 8. Inspection of Eqs. (18) and (20) shows that d_∞, U_{cp}, and V_o all vanish as q approaches q_{L1} but with different exponents. The practical consequence for the observations is that V_o becomes

small for q not extremely close to q_{L1} so that it is not difficult to observe the top and bottom of the lips. For the same deviation from q_{L1}, U_{cp} is relatively large such that the cusp point at the corners of the lips are not easily observed.

It is anticipated that Simpson will complete a manuscript on this research during the next year since he is now carrying out other acoustics research.[30]

D. Observations of Acoustical and Optical Transverse Cusps Produced by Reflection

In the previous Annual Report,[5] experiments are described in which a long tone burst of ultrasound, was reflected from a curved polished metal surface in water. The surface was curved in the generic shape to produce transverse cusp caustic and preliminary plots of the wavefield were obtained by scanning a hydrophone and using the output to modulate the intensity of an oscilloscope. The reflected wavefront has the form of Eq. (16). While those experiments were sufficient to confirm that the wavefield had the anticipated shape of a Pearcey pattern, to facilitate a more quantitative comparison with theory, Carl Frederickson improved the apparatus during the past year including the use of a (Mac. II) graphics display so that theory contours could be superposed on data. A summary manuscript,[31] reproduced here as Appendix B, illustrates the current method and results. It has become only recently apparent that the particular choice of surface parameters used for that experiment was a poor choice for testing the theory. Small errors in surface parameters lead to large errors in wavefield parameters for the surface studied. Consequently, Frederickson has fabricated a new surface for which the wavefield parameters are less dependent on the directly measured surface parameters and improved experiments are under way.

Once a quantitative study of acoustical transverse cusps is successfully completed, it is presently thought that the final aspect of Frederickson's Ph.D. project should be a study of acoustical "lips" or "beak-to-beak" events in acoustical reflections from reported

surfaces.

E. Investigations of Caustics and Associated Wavefields Germane to a Review Chapter

Marston has been preparing a review chapter on "Geometrical and Catastrophe Optics Methods in Scattering" for the series *Physical Acoustics: Principles and Methods* published by Academic Press and Edited by R. N. Thurston and A. D. Pierce. It has been apparent that there are several applications in acoustics for which geometrical methods are either underutilized or for which the derivations in the literature are sketchy at best. In certain cases Marston has carried out new derivations or has examined new applications. Some of the topics included in the chapter in preparation are:

1. A complete re-derivation of the wavefield near the longitudinal (or axial) cusp caustic of a cylindrical wavefront converging to an aberrated focus. The original result by Pearcey[32] (stated without derivation) is correct but the new derivation clarifies the assumptions in Pearcey's result.

2. An apparently novel plot was introduced for displaying the breakdown of Keller's GTD approximation for diffraction by an edge near the shadow boundary. It was subsequently discovered that a similar plot had been only recently introduced in optics.[33]

3. A simple approximation of scattering from a finite tilted circular cylinder was derived from physical optics methods.

4. The construction of two-dimensional wavefronts as involutes of a caustic was reexamined. An application is to the wavefront scattered from a circular cylinder as imaged at the Navy Research Lab by Neubaurer.[34] The prediction is that such wavefront are the involutes of a caustic circle. It appears that this prediction was not previously known.[35]

III. OPTICS OF BUBBLES IN WATER

A. Physical Optics of Bubbles in Water

Previous Annual Reports[4,5] have surveyed research into the physical optics of bubbles in water. Contrary to what may have been anticipated there can be significant errors if purely geometrical methods (adapted to retain phase information) are used to calculate the scattered irradiances. This is because even though bubbles are very much larger than the wavelength of light in water λ_w, the effects of diffraction are significant near caustics and near the critical angle. Physical optics methods are an improvement over purely geometrical methods. In addition to the research summarized below, the following accomplishment is noteworthy: Marston prepared a brief overview of scattering properties for bubbles intended for a general audience.[36]

B. Asymptotic Series for Scattering at the Critical Angle from CAM theory

Some of the motivation for deriving an asymptotic series for scattering at the critical angle was described in the previous Annual Report.[5] Only a brief summary will be given here since the derivation and testing of the series was recently completed by Cleon Dean as part of his Ph.D. Thesis.[24]

The critical scattering angle at $\theta_c = 82.8°$ from an air bubble in water locates the transition from partial to total reflection in elementary geometrical optics. The irradiance scattered into a narrow angular region near the critical scattering is a monotonically increasing function of bubble radius a provided a $>> \lambda_w$ where λ_w is the wavelength of light in water. The asymptotic series for critical angle scattering derived by Dean leads to a simple approximation for the irradiance. It also describes the breakdown of elementary geometrical optics for reflection at the critical angle from a curved interface. The method of derivation extends the complex angular momentum (CAM) theory of Ferrari and
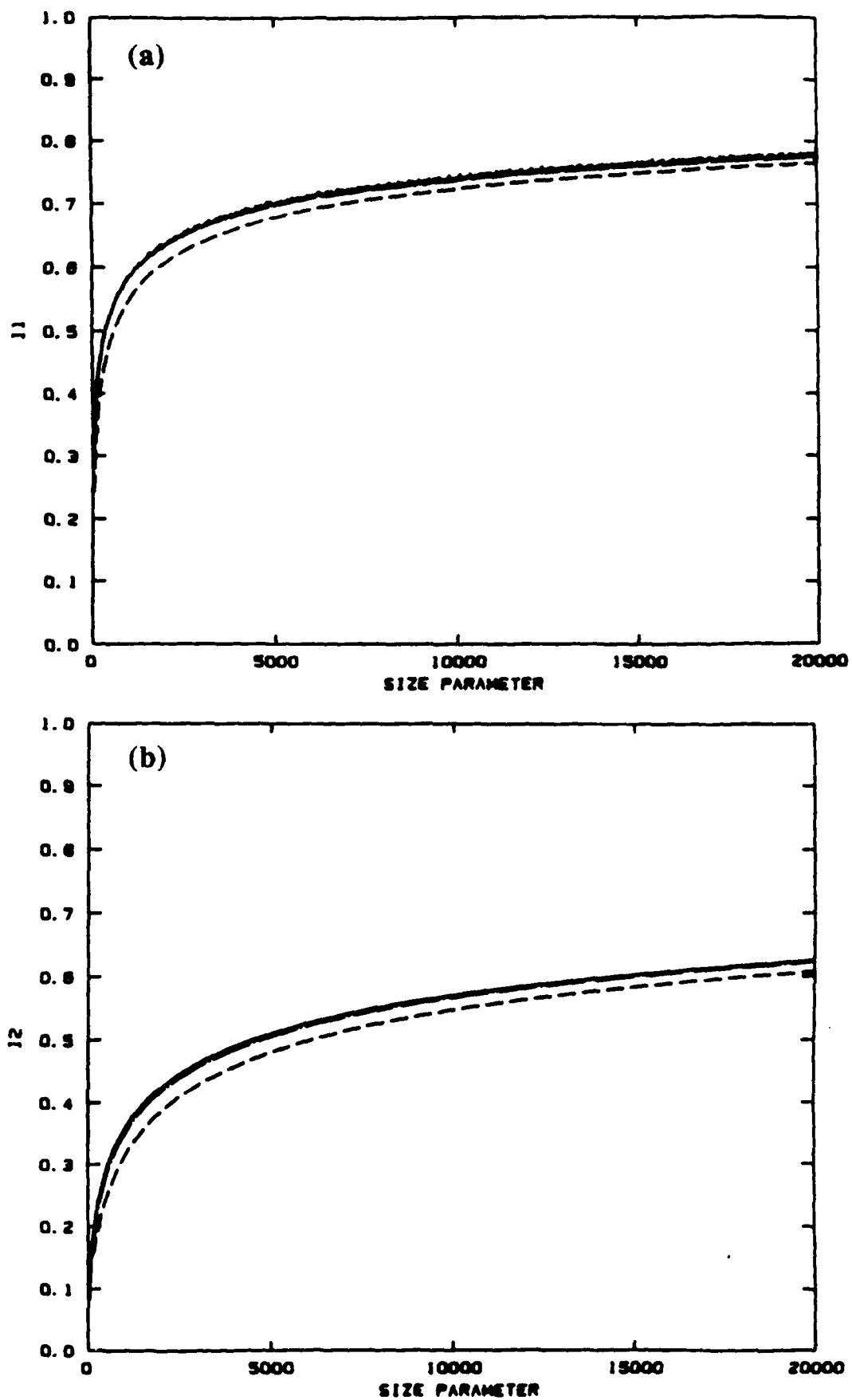
Figure 9

Nussenzveig.[37,38] CAM theory is a modified Watson transformation of the exact Mie series for scattering from a bubble. Dean found that the leading correction to the scattering amplitude relative to that of a perfect reflection is found to be $O(\beta^{-1/4})$ where $\beta = 2\pi a/\lambda_w$ is the size parameter. The series was confirmed by comparison (as a function of β) with smoothed Mie computations. The leading correction is significant for β as large as 20,000, and it is larger when the light is polarized with the E field parallel to the scattering plane than perpendicular to it. Applications to optical bubble sizing have been noted, and the nature of approximations in previous physical optics models of critical angle scattering were clarified.[24]

In the previous work by Ferrari and Nussenzveig,[37,38] the CAM theory lead to integrals which Ferrari evaluated numerically. With a moderate effort, Dean was able to derive an asymptotic series for each of the integrals and hence, a series for the scattering amplitude. This work was only partially supported by this contract.[39] The contribution of the reflected light to the normalized irradiance becomes

$$I_j(\theta_c, \beta) \approx \left| \sum_{q=0}^{M_A} A_{j,q}\, \beta^{-q/4} + \sum_{q=0}^{M_B} B_{j,q}\, \beta^{-q/4} \right|^2, \qquad (21)$$

where $A_{j,0} = B_{j,0} = 1/2$ and the coefficients $A_{j,q}$ and $B_{j,q}$ are complex for $q \geq 1$ and j is a polarization index. Note that $\beta^{-q/4} = 1$ for $q = 0$. Because the analysis leading to $A_{j,q}$ and $B_{j,q}$ is tedious, it was necessary to terminate the series at $M_A = M_B = 2$. (The coefficient of $A_{j,q}$ was incorrectly thought to be $\beta^{-q/6}$ as the time of the previous Annual Report.[6] An error was identified shortly after that report was written and we are confident of the present result because of numerical tests described below.) Some of the noteworthy features evident from inspection of Eq. (21) are (i) $I_j(\theta_c, \beta \to \infty) \to 1$ which is the correct geometric optics limit for total reflection and (ii) the leading correction to the geometric optics limit is $O(\beta^{-1/4})$. This is of fundamental interest since away from special angles, the corrections to geometrical optics are usually $O(\beta^{-1})$.

Figure 9 (a) and (b) show comparisons of Eq. (21) with results from smoothed (exact) Mie theory for a bubble in water where in (a) and (b) the polarization index j is 1 and 2, respectively; these correspond to the scattering of polarized light with the E field perpendicular to and parallel to the scattering plane, respectively. The solid curve in each figure is from Mie theory. The dashed curve is with $M_A = M_B = 1$ in Eq. (21) and the dot-dashed curve is almost indistinguishable from the exact curve. The most difficult part of the analysis was in deriving the correct expressions for $A_{j,2}$ and $B_{j,2}$, smooth functions of the refractive index. The comparisons shown confirms Dean's analysis.

The normalized irradiance I_j is related to the physical irradiance i_j (in W/m^2) by $i_j = i_{inc}(a^2/4R^2)\ I_j$ where R is the distance form the bubble of radius a and i_{inc} is the incident j polarized irradiance. The approximations obtained explain why an angular average of i_j for a scattering angle $\theta \approx \theta_c$ is monotone in a. They provide the theoretical basis for the technique used by Holt[40] to optically detect bubble pulsations.

IV. ACOUSTICAL PHASE CONJUGATION AND ASPECTS OF ACOUSTIC AND WATER WAVE WAVEFRONT REVERSAL

A. Overview of the Project

The project is to investigate physical mechanisms to cause propagating acoustical wavefronts to reverse their direction so as to retrace their path. Such is the case if a "phase conjugate" wave is produced. For laboratory scale experiments it can be convenient to produce a wave of a slightly different frequency which, while nearly reversed in propagation direction, does not exactly retrace the path of the outgoing wave. Various physical mechanisms for doing this with sound, based on nonlinear processes or time dependent variation of medium parameters, are discussed in previous Annual Reports.[4,5]

B. Experiments on Three-Wave Mixing in a Bubble Layer

One of the mechanisms considered for sound is three-wave mixing in a bubble layer

in water. Soviet researchers have claimed to have observed three-wave mixing by that mechanism.[41] Graduate Student Steve Kargl has been carrying out similar experiments with the support of this contract, though with ambiguous results as summarized below and in the previous Annual Report.[5] During the past year, Kargl carried out experiments both at WSU and at the Naval Coastal Systems Center (NCSC) in cooperation with Dr. Douglas G. Todoroff. The results will now be summarized.

At WSU Kargl attempted three-wave mixing in a horizontal bubble layer in a new 500 gallon tank with a water depth of about 6 feet. The bubble layer was trapped against a thin horizontal sheet of Mylar. One significant complication was that the properties of the layer appeared to evolve significantly (due in part to coalescence) during the time a hydrophone was scanned along a line. (This complication makes in no layer meaningful to locate a focus in the reversed wave from an apparent maximum of the wavefield amplitude.) To better understand this problem, Steve examined methods for acoustically characterizing the layer. He is also putting faster interfaces in the digital signal processor (DSP) and affiliated computer so as to speed up data acquisition. (This has been complicated by power supply failures of the DSP which the manufacture has only recently been willing to address following a letter to the Chairman of the Board.) Finally after a delay (from another vendor) Kargl has procured a needed hydrophone for that experiment.

During parts of June and July of 1989, Kargl was attempting similar experiments at NCSC in a 15 ft. x 15 ft. x 8 ft. deep tank.[42a] The experiments were grouped as follows:

1. The first set were similar to experiments tried at WSU where the bubbles layer was trapped against a thin horizontal sheet of Mylar. In addition to the large size of the tank, another advantage of this facility is the ease by which attenuation measurements could be obtained for transmission through the layer. Measurements showed a maximum attenuation near 50 kHz. Layers were subjected to a strong 400 kHz pump signal and a ~ 350 kHz probe and a reversed wave at the difference

frequency (at or close to 50 kHz) was searched for. No unambiguous reversed wave focus was located and signals of the expected magnitude were not observed. It is note worthy however, that real time signal averaging was not used.

2. The second set of experiments were done with a layer of freely-rising larger bubbles for which the resonance was in the 20 to 30 kHz range. The pump and probe signals were lower in frequency, the pump typically being ~ 100 kHz. The results were ambiguous as in the first set. The parameters for this set were similar to those in the Soviet experiments except with stronger pump and probe signals and a more sensitive hydrophone. Kargl's negative results cast doubt on the interpretation of the Soviet research.[41]

In spite of the results, the joint effort between the NCSC and WSU projects was mutually beneficial.

Kargl is presently setting up experiments at WSU to resolve an important related physics issue. If one monitors the difference frequency sound radiated by a single bubble, how does that radiation build up when the pump and probe signals are in the form of bursts? Such measurements will be helpful in determining how long the pump and probe bursts will need to be in three-wave mixing experiments in order to simulate the steady-state condition assumed in calculations such as those given in Ref. 5 and 41. While Atchley et al.[42b] appear to have detected the difference frequency response of a bubble, they did not report observations of the response to bursts.

The results of our experiments with single bubbles subjected to bursts will affect the design of subsequent experiments with layers. Kargl's Ph.D. thesis effort is split between this problem and research on applying ray methods to scattering from elastic objects as described in Sec. IB-D.

C. Phase Conjugation and Wavefront Reversal of Ripples on a Water

Tank.

At present, the expressions derived[4,5] for the focal location of reversed waves are without clear verification from experiments. Two-dimensional waves represent a special case of those expressions so that observations for such waves would be germane to verification. Instead of two-dimensional sound waves, a M.S. degree candidate, J. Michael Winey is preparing to look for wavefront reversal in a ripple tank. The depth h of the water in the tank is set to 5 mm such that the dispersive effects of surface tension and gravity nearly cancel[43] if the frequency is less than about 10 Hz. Consequently a tone burst of such waves should spread out only weakly with propagation. A number of parametric mechanisms are possible for producing a (reversed) difference-frequency wave, the simplest being the modulation of the height of a slanted boundary.

The status of the experiment is as follows. During the approximately 1 1/2 months which Winey has worked on the experiment he has built a point source for ripple tone bursts and has been able to detect the ripples optically. The source is a partially immersed cone with a narrow apex angle which is moved vertically by a moving-coil loud speaker. To detect the waves a dye is put in the water and the attenuation of a narrow laser beam passing vertically through the water is measured. The attenuation varies with depth. The upper and lower records of Fig. 10 show three-cycle bursts having frequencies of 7 Hz and 12 Hz, respectively. The burst near the center of each trace has propagated directly 16 cm from the source to the optical receiver. The weaker burst near the end of the trace is a wall reflection with a total propagation distance of about 30 cm. There is also a signal near the beginning of each trace attributed to a direct electrical coupling. These experiments were carried out in a 25 cm x 50 cm glass bottomed aquarium.

When Winey, who is presently supported by a teaching assistantship, returns to the project, plans are for him to build a much larger ripple tank (roughly 1 m x 2 m) in which to attempt parametric wavefront reversal experiments. The source and detector techniques described above will be used together with a localized high frequency of the depth. An
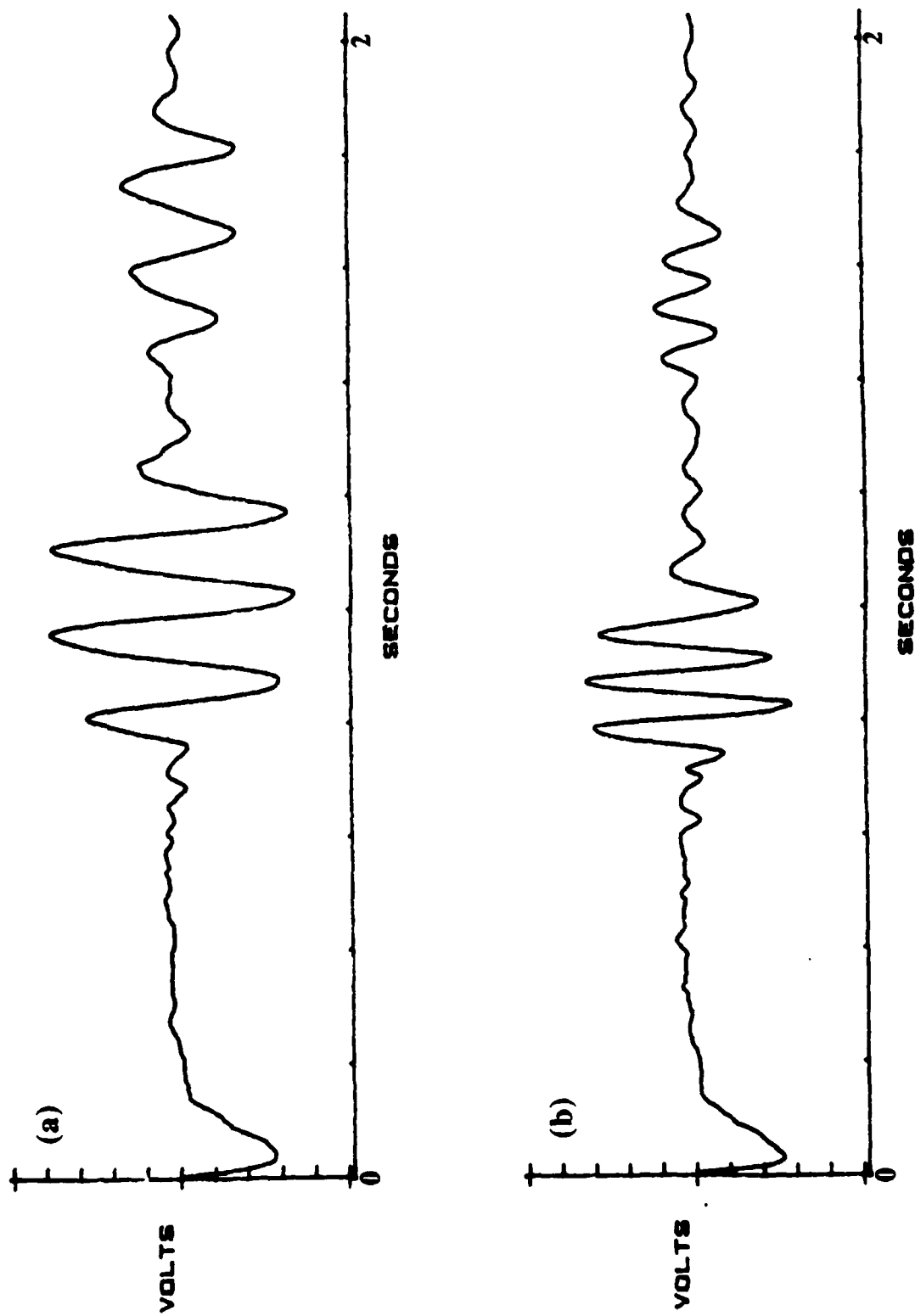
(a)

VOLTS

SECONDS

(b)

VOLTS

SECONDS

Figure 10

order-of-magnitude estimate of the reversed wave magnitude indicates the experiment is worth attempting.

V. RESPONSE OF THE WAKE OF A CIRCULAR CYLINDER TO FORCED TORSIONAL OSCILLATIONS: WAVES ON SHEAR LAYERS AND VORTICES

A. Overview of the Project

The shedding of vortices in flow past bluff bodies is a long standing problem having applications as well as fundamental significance.[44,45] The understanding and control of vortex shedding has potential applications for drag reduction, control of structural vibrations, and noise control. With the partial support of the contract,[46] a Ph.D. candidate; J. R. Filler, has been studying experimentally a novel method for affecting vortex shedding and waves on shear layers which separate from a cylinder. The response to small amplitude torsional oscillations of the cylinder is measured as will be discussed subsequently and has been studied with flow visualization. At the time these experiments were initiated in 1988, we were unaware of any prior study of the response to torsional oscillations, though several groups had studied effects of transverse oscillations (e.g., Ref. 45). Following our initial observations we became aware of current[47] and previous[48] observations of effects of torsional oscillations. Our work, however, measures properties and flow regimes not previously studied. It makes use of real time signal processing techniques similar to ones used in basic acoustics research.

B. Forcing of Waves on Shear Layers and Primary and Secondary Vortices

Figure 11 is a diagram of the apparatus. The cylinder is immersed in a 69 ft long open channel water flume. In the absence of the cylinder the flow is uniform with a velocity U_0 which is typically 5 cm/s $\approx$ 2 in/s. The Reynolds number, which should characterize the flow if it were purely two-dimensional, is defined as $Re = U_0 d / \nu$ where d
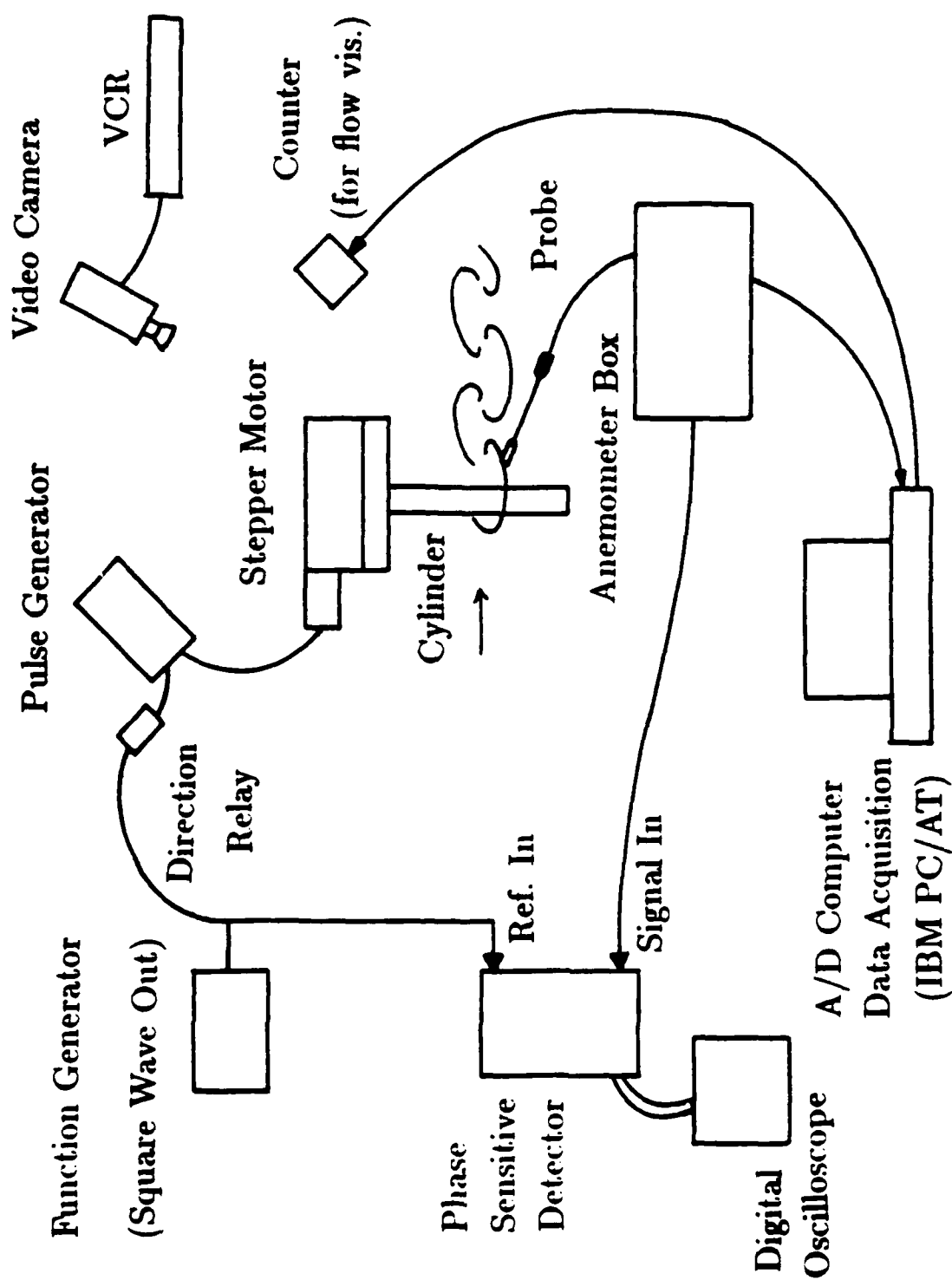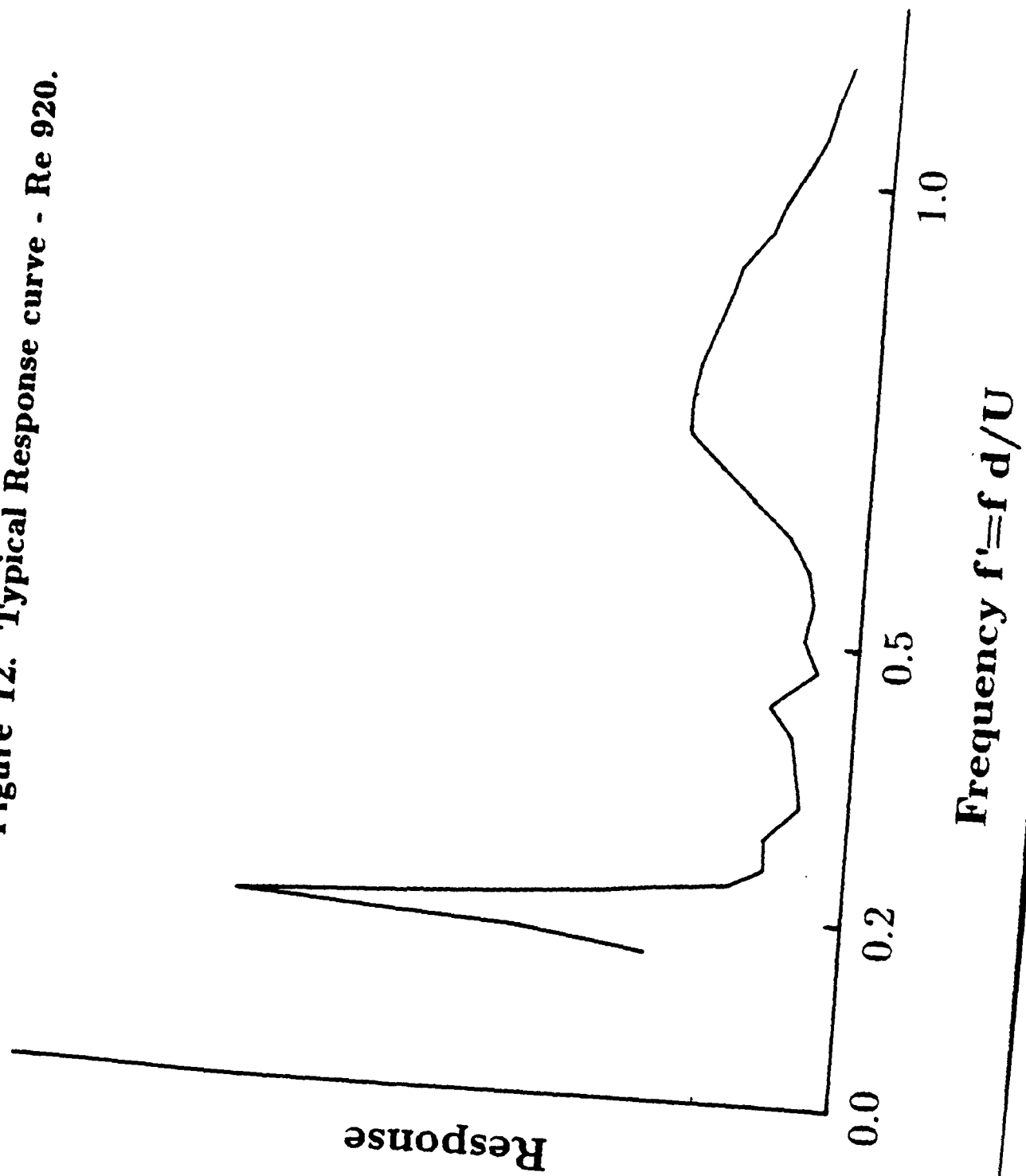
Figure 11. Experimental set up.

is the cylinder diameter and ν is the kinematic viscosity of water. For the experiments summarized below Re was in the range 250 to 1200 and d was typically 1.27 cm. It is well known that in this range, the flow along the surface of a stationary cylinder separates from each side to produce a pair of free shear layers. (A shear layer is characterized by a rapid change in the tangential velocity, in this case over a distance of a few mm.) An interaction of the shear layers contributes to the formation of the von Karman vortex street down stream from the cylinder. The frequency of the naturally occurring vortex pairs is f_S where $f_S = U_0 S/d$ and S is the nondimensional Strouhal number which typically has a value ≈ 0.2. The typical magnitude of f_S was 1 Hz.

In the experiments the cylinder was driven by a stepper motor such that the angular velocity was approximately a square wave function of time. Relative to the laboratory frame, the tangential velocity of the surface of the cylinder had a fundamental component $U_T \cos(2\pi ft)$. The oscillation amplitude was sufficiently small that U_T/U_0 was typically $\lesssim 0.02$. A hot film anemometer was placed in the wake downstream a distance typically 0.5 to 1 d past the back end of the cylinder. The anemometer was laterally positioned to lie in (or close to) the separated shear layer. Small changes in the anemometer voltage $V_a(t)$ were approximately linearly related to small changes in the velocity magnitude U at the anemometer. To facilitate the discussion which follows it is convenient to decompose $V_a(t)$ as

$$V_a(t) = V_0 + V_1 \cos(2\pi ft + \phi) + V_r(t), \tag{22}$$

where V_r is a zero-mean residue having only insignificant spectral components at the driven frequency f. The values for V_1 and ϕ were measured with a phase sensitive detector ("lock-in amplifier") having a long integration time (typically ≈ 100 sec.). For a fixed f, the measured value of V_1 increases with the oscillation amplitude U_T until the

Figure 12. Typical Response curve - Re 920.

Response

Frequency f'=f d/U

36

response saturates: V_1 is related to the velocity fluctuations in the wake driven by the cylinders torsional oscillations. The velocity change may, however, be only roughly linear in V_1. With U_T fixed, f was stepped through a range of values and $V_1(f)$ and $\phi(f)$ were measured.

Figure 11 shows a representative response curve for V_1 as a function of the dimensionless forcing frequency $f' = fd/U_o$. It is for $Re = 920$. The peak near $f' = 0.2$ is such that f is close to the natural shedding frequency f_S. It appears to be associated with the forcing of the shedding Strouhal vortices. For $Re \gtrsim 500$, a broader peak is observed at a somewhat higher f'; in Fig. 11 this peak is centered near $f' \approx 0.8$. This peak appears to be associated with waves which are convected along the free shear layer at a phase velocity of roughly the mean velocity $\bar{U}$ of the shear layer. Experimental evidence for the latter include measurements of $\phi(f)$ showing that $d\phi/df$ is roughly constant in this region having a value roughly consistent with the estimated $\bar{U}$ and the propagation distance along the (curved) shear layer from the separation point of the cylinder. Other evidence includes flow visualization experiments mentioned below.

The existence of the broad high-frequency peak in Fig. 12 may have been anticipated from a calculation by Monkewitz and Heurre[49,50] which partially motivated this measurement. They calculated the response of a free initially flat shear layer to a velocity perturbation of frequency f_p. They found that the perturbation can be amplified with propagation along the layer and that there is a most amplified frequency f_{pm} such that $f_{pm} \approx 0.032 \bar{U}/\theta$ where θ is the local momentum thickness of the layer. Furthermore, for sufficiently large f_p, the perturbation is attenuated with propagation. Filler's estimates[51] of f_{pm} for the shear layers which separate from the cylinder place f_{pm} in the general region of the broad maximum in Fig. 12. Consequently there is theoretical reasons for interpreting that peak as the most amplified frequency of the shear layer. It is also known that the most-amplified perturbation can roll-up the shear layer to produce vortices. Such vortices which

grow in separated shear layers of cylinders are sometimes known as secondary vortices[52] and there is some evidence that they can affect the downstream formation of Strouhal (or primary) vortices. Filler visualized the shear layer response by injecting dye and found that high frequency torsional oscillations of the cylinder can enhance what appears to be the production of shear layer vortices.

The experiments shed light on several other local flow phenomena; for example, there is a jump in the phase ϕ as f is scanned through the Strouhal peak. Filler is at the time of this writing preparing a Ph.D. thesis which describes and analyzes his experiments. There may be implications for active control of flow past cylinders.

VI. REFERENCES

1. V. A. Borovikov and N. D. Veksler, "Scattering of sound waves by smooth convex elastic cylindrical shells," Wave Motion **7**, 143-152 (1985).

2. K. L. Williams and P. L. Marston, "Backscattering from an elastic sphere: Sommerfeld-Watson transformation and experimental confirmation," J. Acoust. Soc. Am. **78**, 1093-1102 (1985); **79**, 2091(E) (1986).

3. K. L. Williams and P. L. Marston, "Synthesis of backscattering from an elastic sphere using the Sommerfeld-Watson transformation and giving a Fabry-Perot analysis of resonances," J. Acoust. Soc. Am. **79**, 1702-1708 (1986).

4. P. L. Marston, "Research on Acoustical Scattering, Diffraction Catastrophes, Optics of Bubbles, Photoacoustics, and Acoustical Phase Conjugation," Annual Summary Report, issued Sept. 1987 (Defense Technical Information Center, AD-A185785) 84 pages.

5. P. L. Marston, "Research on Acoustical Scattering, Diffraction Catastrophes, Optics of Bubbles, and Acoustical Phase Conjugation," Annual Summary Report, issued October 1988 (Defense Technical Information Center, AD-A2011451) 52 pages.

6. P. L. Marston, "GTD for backscattering from elastic spheres and cylinders in water, and the coupling of surface elastic waves with the acoustic field," J. Acoust. Soc. Am. **83**, 25-37 (1988).

7. S. G. Kargl and P. L. Marston, "Observations and modeling of the backscattering of short tone bursts from a spherical shell: Lamb wave echoes, glory, and axial reverberations," J. Acoust. Soc. Am. **85**, 1014-1028 (1989).

8. See preprint in Appendix A.

9. L. B. Felsen, J. M. Ho, and I. T. Lu, "Three dimensional Green's function for fluid-loaded thin elastic cylindrical shell: Alternative representations and ray acoustic forms," J. Acoust. Soc. Am. (to be published).

10. L. B. Felsen and I. T. Lu, J. Acoust. Soc. Am. **86**, 360-374 (1989).

11. A. D. Pierce, "Wave propagation and excitation on thin-walled elastic cylinders," in *Elastic Wave Propagation*, IUTAM Symposium, Galway, Ireland, ed. by M. F. McCarthy and M. A. Hayes (Elsevier, NY, 1989).

12. P. L. Marston, "Phase velocity of Lamb waves on a spherical shell: Approximate dependence on curvature from kinematics," J. Acoust. Soc. Am. **85**, 2663-2665 (1989).

13. S. G. Kargl and P. L. Marston, "GTD synthesis of Lamb wave contributions to the total scattering cross section for an elastic spherical shell," J. Acoust. Soc. Am. (submitted).

14. H. M. Nussenzveig, *Causality and Dispersion Relations* (Academic, New York, 1972).

15. S. G. Kargl and P. L. Marston, "Quasiperiod of variations in the backscattering and total cross sections of spherical shells," to be presented at Fall 1989 ASA meeting.

16. P. L. Marston and S. G. Kargl, "Elastic Surface Wave Contributions to Backscattering from Smooth Objects Described by a Generalization of GTD," *Oceans' 89 Proceedings* (IEEE, New York, 1989) pp. 1194-1198.

17. It is anticipated that Kargl will complete manuscripts on this aspect of his thesis work during the next year.

18. T. Pialucha *et al.*, Ultrasonics **27**, 270-279 (1989).

19. L. Flax, G. C. Gaunaurd, and H. Überall, "Theory of Resonance Scattering," in *Physical Acoustics*, edited by W. P. Mason and R. N. Thurston (Academic, New York, 1981), Vol. 15, pp. 191-294.

20. Ref. 14 and N. G. van Kampen, Phys. Rev. **89**, 1072-1079 (1953).

21. P. L. Marston and E. H. Trinh, Nature **312**, 529-531 (1984).

22. P. L. Marston, "Cusp diffraction catastrophe from spheroids: generalized rainbows and inverse scattering," Opt. Lett. **10**, 588-590 (1985).

23. P. L. Marston, "Transverse cusp diffraction catastrophes: Some pertinent wavefronts and a Pearcey approximation to the wavefield," J. Acoust. Soc. Am. **81**, 226-232 (1987).

24. C. E. Dean, "Analysis of Scattered Light: I. Asymptotic Series for Critical Angle Scattering from Bubbles; II. The Opening Rate of the Transverse Cusp from Oblate Drops," Ph.D. Thesis, Washington State University, 1989.

25. P. L. Marston "Geometrical and Catastrophe Optics Methods in Scattering," in

preparation for *Physical Acoustics: Principles and Methods* (Academic Press).

26. J. A. Kneisly, J. Opt. Soc. Am. **54**, 229-235 (1964).

27. P. L. Marston, C. E. Dean, and H. J. Simpson, "Light Scattering from Spheroidal Drops: Exploring Optical Catastrophes and Generalized Rainbows," *Proceedings of the Third International Colloquium on Drops and Bubbles* (A.I.P., at press).

28. J. F. Nye, "Rainbow scattering from spheroidal drops—an explanation of the hyperbolic umbilic foci," Nature (London) **312**, 531-532 (1984).

29. H. J. Simpson, "The Lips Event for Light Backscattering from Levitated Water Drops," M. S. degree project report, Washington State University Physics Department (July 1988).

30. Simpson is presently working on an acoustical 4-wave mixing experiment supported by ONR grant N00014-89-J-3088.

31. C. K. Frederickson and P. L. Marston, "Transverse Cusp Diffraction Catastrophes Produced by Reflection Ultrasonic Tone Bursts from Curved Surfaces," in *Proceedings of the IUTAM Symposium on Elastic Wave Propagation and Ultrasonic Nondestructive Evaluation*, ed. by S. K. Datta *et al.* (Elsevier, at press).

32. T. Pearcey, "The structure of an electromagnetic field in the neighborhood of a cusp caustics," Philos.. Mag. **37**, 311-317 (1946).

33. Y. A. Kravtsov, "Rays and caustics as physical objects," in *Progress in Optics*, Vol. XXVI (Elsevier, Amsterdam, 1988).

34. W. G. Neubauer, J. Acoust. Soc. Am. **48**, 1135-49 (1970).

35. W. G. Neubauer (private communications).

36. P. L. Marston, "Light Scattering from Bubbles in Water," *Oceans' 89 Proceedings* (IEEE, New York, 1989) pp. 1186-1193; research partially supported by the Naval Ocean Research and Development Activity.

37. N. F. Ferrari, Jr., "Espalhamento de Mie na Vizinhanca do Angulo Critico," Ph.D. thesis, University of São Paulo Brazil, 1983 (in Portuguese).

38. H. M. Nuzzenzveig, "Recent developments in high-frequency scattering," Rev. Bras. Fiz. (Brazilian Reviews of Physics, special issue) 302-320 (1984).

39. From September 1987 through February 1988, the work of Cleon Dean on this project was supported entirely by a $10,000 contract (N00014-87-K-6008) with the Naval Ocean Research and Development Activity.

40. R. G. Holt, "Experimental Observation of the Nonlinear Response of Single Bubbles to an Applied Acoustic Field," Ph.D. Thesis, Univ. Mississippi 1988.

41. L. M. Kustov, V. E. Nazarov, and A. M. Sutin, "Nonlinear sound scattering by a bubble layer," Sov. Phys. Acoust. **32**, 500-503 (1986); "Phase conjugation of an acoustic wave at a bubble layer," *ibid.* **31**, 517-518 (1985).

42a. Equipment purchased by the present contract was moved to NCSU and used in this experiment though funds for Kargl's salary and expenses were paid through an Intergovernmental Personnel Act agreement with NCSC.

42b. A. Atchley *et al.*, J. Acoust. Soc. Am. Suppl. **85**, S5 (1989).

43. J. Lighthill, *Waves in Fluids* (Cambridge, U.P., 1978) pp. 224-227.

44. R. King, "A review of vortex shedding research and its application," Ocean Engng **4**, 141-1171 (1977).

45. D. J. Olinger and K. R. Sreenivasen, Phys. Rev. Lett. **60**, 797-800 (1988).

46. Albrook Hydraulics Lab at W.S.U. supplies its flow facility at no charge as well as the principal financial support for Filler.

47. P. T. Tokumaru and P. E. Dimotakis, "Rotary Oscillation Control of a Cylinder Wake," AIAA paper 89-1023.

48. A. Okajima *et al.*, "Viscous flow around a rotationally oscillating circular cylinder," Report No. 532, Institute of Space and Aeronautical Science, University of Tokyo (1975).

49. P. A. Monkewitz and P. Huerre, "Influence of velocity ratio on the spatial instability of mixing layers," Phys. Fluids **25**, 1137-1143 (1982).

50. C. M. Ho and P. Huerre, "Perturbed Free Shear Layers," Ann. Rev. Fluid Mech. **16**, 365-424 (1984).

51. J. R. Filler, "Small and Large Scale Vortex Shedding in the Wake of a Circular Cylinder," Dept. of Civil and Environmental Engineering, W.S.U., 1988.

52. T. Wei and C. R. Smith, "Secondary vortices in the wake of circular cylinders," J. Fluid Mech. **169** (1986).

42

APPENDIX A

RAYLEIGH, LAMB, AND WHISPERING GALLERY WAVE CONTRIBUTIONS TO BACKSCATTERING FROM SMOOTH ELASTIC OBJECTS IN WATER DESCRIBED BY A GENERALIZATION OF GTD

Philip L. MARSTON,* Steven G. KARGL,* and Kevin L. WILLIAMS†

*Department of Physics   †Applied Physics Laboratory
Washington State University   University of Washington
Pullman, Washington 99164   Seattle, Washington 98195

Surface guided elastic waves on objects in water can significantly contribute to the
scattering of sound. The present research concerns the development and testing of a
quantitative ray representation of such contributions to backscattering from smooth
elastic objects. Resulting resonance structure is compared with that from the exact
partial wave series for solid and hollow spheres. Experimental tests used short tone
bursts so that different contributions were separated in time. The analysis concerns
leaky guided waves having phase velocities exceeding that of water.

1. INTRODUCTION

The usual geometrical theory of diffraction (GTD) gives a ray representation of scattering
amplitudes for rigid objects [1] and is generalizable to certain bulk-transmitted-wave contributions
for solid elastic objects [2]. One of the difficulties in extending GTD methods to elastic objects
such as shells in water is that the contributions due to *surface guided elastic waves* (SEW) can be
important. Examples of SEW include leaky Lamb waves on shells and Rayleigh and whispering
gallery waves on spheres. The extension of GTD to represent backscattering from such objects
should facilitate the partitioning of complicated high-frequency scattering problems into geometry
and the local mechanics of the interaction of the sound field in water with the SEW. Such an
extension should give a simple and *quantitative* understanding of the scattering process which could
be useful both for inverse problems and for predicting how changes in an object will affect the
scattering. The present paper summarizes the development of such an extension, directs the reader
to detailed literature, and gives novel relevant derivations for amplitudes and phases.

Figure 1 illustrates a generic problem of interest. A plane wave is incident on a smooth empty shell
having a circular profile. One contribution to backscattering is due to specular reflection from the
region near point C; however, that is not the contribution of primary concern here. The incident
sound wave excites an elastic surface wave at point B which repeatedly circumnavigates the object
radiating sound back towards the source from point B'. A heuristic model of this scattering
process was put forth by Borovikov and Veksler [3]. In their analysis, however, the coefficient
which describes the coupling of SEW with the acoustic field in water was determined by a fitting
procedure. A rigorous analysis of backscattering from solid elastic spheres was carried out by
Williams and Marston [4,5] based on the Watson transformation of the exact partial-wave series.
That analysis gives a virtually exact expression for the required complex coupling coefficient G_l
for the specific case of a solid elastic sphere. (The dependence of G_l on physically relevant
parameters was, however, obscure.) That analysis predicts that the contribution to the form
function for the farfield backscattering amplitude due to the lth class of SEW is simply

$$ f_l = \frac{-G_l \exp\left[-2(\pi-\theta_l)\beta_l + i\eta_l\right]}{\left[1 + j\exp(-2\pi\beta_l + i2\pi kac/c_l)\right]}, \quad \frac{p_{sca}}{p_{inc}} = \frac{fa\exp[i(kr - \omega t)]}{2r} \qquad (1,2) $$

where c and k are the sound velocity and wavenumber in the surrounding water, a is the sphere's radius, η_l is a propagation phase delay and $j = 1$ for a sphere. Parameters which describe the surface wave are the phase velocity c_l and radiation damping parameter β_l (in np/radian). As reviewed in Sec. 3, f_l is part of the total form function f which relates the scattered and incident pressures by Eq. (2). A trace-velocity matching condition gives for $c_l > c$

$$\theta_l = \arcsin(c/c_l) , \quad \eta_l = 2ka\left[(c/c_l)\left(\pi - \theta_l\right) - \cos\theta_l\right] - (j + 1)\pi/4 \quad (3a,b)$$

Equation (1) predicts a sequence of resonance peaks and is like the form used to describe Fabry-Perot resonators [5]. Superposition of such contributions for Rayleigh and whispering gallery waves with a specular reflection term synthesize accurately the backscattering computed directly from the partial-wave series for a solid sphere [5,6]. [It may be shown [6] that Eqs. (1) and (3) apply also to right circular cylinders by taking $j = -1$ though the exact expression for the coefficient G_l was not obtained.] Measurements of backscattering of short tone bursts due to Rayleigh waves on a solid sphere, reviewed below in Sec. 2, were also described by the theory [4,7].

To facilitate the description of how f_l depends on the interaction of the sound wave in water with the surface wave, it was desirable to express G_l in terms of the SEW properties c_l and β_l. An analysis [6] yields the following approximations for the sphere and circular cylinder cases,

$$|G_l^{sp}| \approx 8\pi\beta_l \, c/c_l, \quad |G_l^{cy}| \approx 8\pi\beta_l \, /(\pi ka)^{1/2}, \quad (4,5)$$

where a is the radius of the cylinder. As discussed in Sec. 4, where the phase of G_l is also considered, these approximations were derived by comparing the form of Eq. (1) near a weakly damped resonance peak with standard (approximate) results [8] of resonance scattering theory (RST). It should be emphasized that Eq. (4) is much simpler than the exact result known for solid spheres [4] since the dependence on β_l is evident. The connection between (4) and (5) follows from ray arguments summarized in Ref. 6 and below in Sec. 4. The original confirmation of Eqs. (4) and (5) was based on numerical comparison with the exact $|G_l|$ for solid spheres [4] and Veksler's fitted result for symmetric Lamb waves on a hollow cylinder [3]. The simple form of Eqs. (4) and (5) facilitate quantitative ray tracing for surface wave contributions without use of a fitting procedure and should simplify the procedure for revising Eq. (1) for other objects. The important SEW parameters for a given frequency and radius of curvature a were originally obtained by locating the complex root v of $D_v(ka) = 0$ associated with the lth SEW where $D_n(ka)$ is the denominator of the nth partial wave in the exact series [6]. For a leaky Lamb wave on a shell, c_l can sometimes be approximated from flat plate results by introducing curvature corrections [9].

2.   MEASURED BACKSCATTERING OF SHORT TONE BURSTS FROM A SHELL AND A SOLID SPHERE

This section reviews theoretical results and supporting experiments from Refs. 4, 7, and 10 concerning the backscattering of short tone bursts. The wave incident on the spheres was approximately a 3 or 4 cycle sine wave burst from a distant source with a frequency $\omega/2\pi$ as low as 300 kHz. For the experiments with a solid tungsten carbide sphere [4,7], Fig. 1 is applicable with $b = 0$ and the major SEW contribution was due to a leaky Rayleigh wave designated by $l = R$. Figure 2(a) shows the observed sequence of backscattered echoes for such a sphere with $a = 1.27$ cm and $ka = \omega a/c = 43.2$. The initial response labeled S is due to the specular reflection from the region near C in Fig. 1. The first echo labeled R is due to a Rayleigh wave which partially circumnavigates the sphere (from B to B' in Fig. 1) and will be assigned an index $m = 0$. The subsequent echoes are due to energy radiated by the Rayleigh wave burst as it circumnavigates the sphere m times, $m = 1, 2, \ldots$. Echoes with large m are reduced in amplitude by radiation damping. The pressure amplitude of a distinct echo due to the lth class of surface wave has the predicted form [7,10]
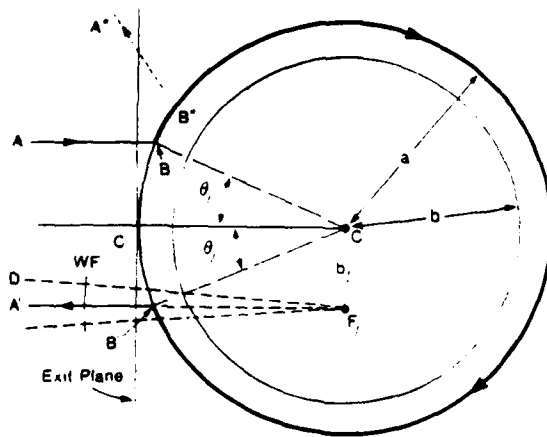
FIGURE 1

Ray diagram for contributions to backscattering
due to a surface wave (of type l) excited near B
on an elastic sphere or cylinder. WF designates
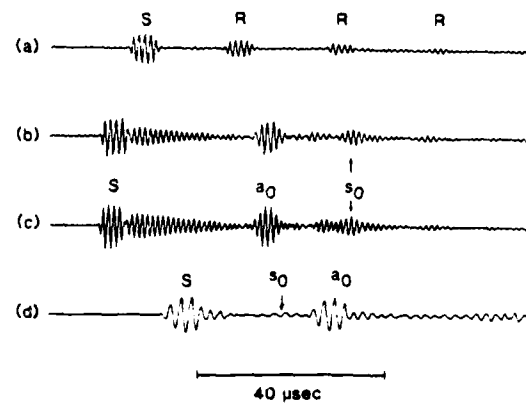part of the outgoing wavefront.

FIGURE 2

Measured echoes for backscattering from solid
(a) and hollow (b-d) spheres. S denotes the
specular echo. It is followed in (b) and (c) by a
tail; here ka is near the thickness resonance and
the onset of the $l = s_1$ wave.

$$|p_{ml}| = |p_i| A_{ml} a/2r, \qquad A_{ml} = |G_l| \exp\left[-2(\pi-\theta_l)\beta_l - 2\pi m\beta_l\right]|J_0(u) - i\beta_l\gamma J_1(u)|, \qquad (6,7)$$

where J_0 and J_1 are Bessel functions evaluated at $u = ka\,\gamma c/c_l$; $|p_i|$ is the amplitude of the
incident wave, γ is the backscattering angle, and r is the distance from the center of the sphere.
(The normalization in Eq. (6) is such that specular reflection from a large fixed rigid sphere
produces a wave whose amplitude is $|p_i|\, a/2r$.) For scattering in the exactly backward direction, γ
$= 0$ so that $|J_0(u) - i\beta_l\,\gamma J_1(u)| = 1$. Measured amplitudes with $\gamma = 0$ agreed with predictions for
$m = 0$ and 1 over a range of ka [4]. As γ is shifted away from $\gamma = 0$, $|p_{ml}|$ decreases which is a
manifestation of glory scattering [7]. The reduced amplitude was nearly proportional to $|J_0(u)|$
since $|\beta_R\,\gamma J_1(u)| \ll 1$.

Backscattering was measured from an empty stainless steel spherical shell [10]. The shell
dimensions were: radius $a = 19.05$ mm; thickness $h = a - b = 3.1$ mm; and $b/a = 0.838$. Figure
2(b), (c), and (d) are representative records for the hydrophone placed on the backward axis for ka
of 64.7, 68.8, and 36.4, respectively. For these ka, the SEW contributions are primarily the
lowest antisymmetric (or flexural) and symmetric leaky Lamb waves for which case l becomes a_0
and s_0, respectively. The identification of the $m = 0$ contributions in Fig. 2 is in accordance with
their arrival time relative to the specular echo S. The times were in good agreement with delays
based on group velocities c_{gl} and modeled path lengths. From echo amplitudes, A_{0l} of Eq. (6)
was measured and compared with the predictions of Eqs. (4) and (7). This was done with $\gamma = 0$
for several ka from 24 to 75 except where a_0 and s_0 echoes overlapped or were weak. The
agreement with theory was good for a laboratory scale experiment of this type. Detailed off-axis
measurements of A_{0l} with $l = a_0$ were obtained for ka $= 24.3$ where the on-axis echo was
strong ($A_{0l} = 1.1$). These measurements were in excellent agreement with Eqs. (4) and (7) and
clearly display a minimum near the γ of the first zero of $J_0(ka\,\gamma c/c_l)$. Note that Eq. (7) neglects
the reduction in echo amplitude due to dispersion. For the conditions of the experiments the
reduction was estimated to be negligible [10].

3. SIMPLE APPROXIMATE SYNTHESIS OF BACKSCATTERING FORM FUNCTIONS

The synthesis of the form function for spheres previously confirmed for tungsten carbide [5] was
greatly simplified and applied to solid and hollow spheres. In Eq. (1), the approximation $G_l \approx
8\pi\beta_l c/c_l$ was used from Eq. (3) and an approximation (see Sec. 4) yielding arg $(G_l) \approx 0$. The
specular contributions to backscattering may be approximated as [3,4]

45

$$f_S^{(solid)} = r\exp(-i2ka), \qquad r = (\rho_E c_L - \rho c)/(\rho_E c_L + \rho c),\qquad(8,9)$$

$$f_S^{(shell)} = \mathcal{R}\exp(-i2ka) + f_{Scc}, \qquad \mathcal{R} = r - \frac{(1-r^2)\exp(i2k_L h)}{1 - r\exp(i2k_L h)}\qquad(10,11)$$

where ρ_E and c_L are the density and bulk longitudinal velocity of the solid, $\mathcal{R}$ is the complex reflection coefficient of a vacuum-backed flat plate of thickness h, $k_L = \omega/c_L$, and f_{Scc} is a curvature correction. The expression for $\mathcal{R}$ may be derived by summation of the ray geometric series for reverberations in a plate [3]. As was done in Ref. 3 for cylinders, the curvature correction will be omitted in the synthesis which follows so that for the shell $|f_S| = |\mathcal{R}| = 1$. The ray approximations to the total form functions for the solid and shell spheres are

$$f = f_S + f_{l=R} + f_{l=WG1}, \qquad f = f_S + \sum_{n=0}^{N_a-1} f_{l=a_n} + \sum_{n=0}^{N_s-1} f_{l=s_n},\qquad(12,13)$$

where WG1 designates the slowest whispering gallery wave and the number N_a and N_s of antisymmetric and symmetric Lamb wave contributions depends on ka through the existence of roots of $D_V(ka) = 0$. Figure 3 and 4 compare resulting $|f|$ with exact values from the partial wave series. The synthesis is verified in each case. The material parameters are as listed in Ref. 5 and 10, respectively, and for the shell $b/a = 0.838$. Notice that in addition to parameters in f_S, the material parameters only enter through the c_l and β_l and these are given from roots v_l of $D_V(ka) = 0$. The finest structure in Fig. 3 is due to WG wave resonances and fine structure not synthesized is due to higher WG modes. In Fig. 4, it is due to the s_0 wave resonances since β_l is less than that for $l = a_0$ in this region and $N_s = N_a = 1$. Whether a resonance causes a dip or a peak in $|f|$ can be understood from the relative phases of the contributions [5]. The spacing Δka of resonances for a given class of weakly dispersive SEW is roughly c_{gl}/c.
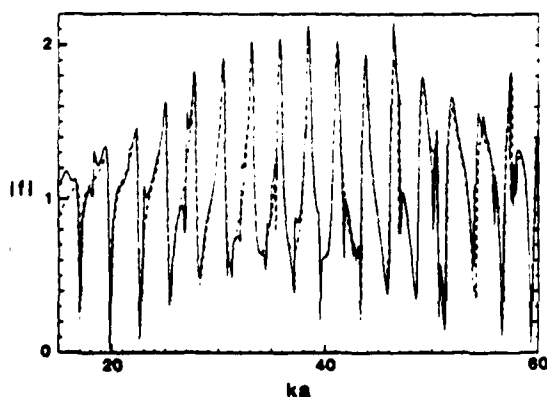

FIGURE 3
Form function for steady-state backscattering from a tungsten carbide sphere: exact (solid curve) and synthesis from Eq. (12), (dashed).
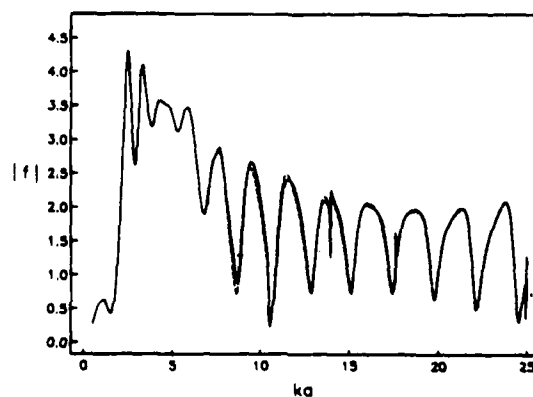
FIGURE 4
As in Fig. 3 but for a stainless-steel spherical shell and the synthesis (dashed) from Eq. (13), includes $l = a_0$ and s_0 Lamb contributions.

The synthesis is terminated in Fig. 4 at $ka = 7$ since $c_l < c$ at lower ka for $l = a_0$. Felsen et al. [11] have developed a ray representation for cylinders which should facilitate the description of scattering contributions of subsonic or "trapped" waves such as flexural waves having $c_l < c$. Unlike Fig. 1, the coupling with the sound field involves tunneling through an evanescent region. Some *other* limitations of our approximations for the shell are found by extending the comparison in Fig. 4 to higher ka. The omitted f_{Scc} is significant near the lowest thickness resonance which occurs at $ka = \pi c_L a/ch = 77$. While the synthesis up through $ka = 100$ correctly describes

additional fine structure due to the a_1 wave (which occurs when N_a becomes 2 for $ka > 40$), the ka region near 70 where N_s becomes 2 is not well approximated by Eq. (13). At the cutoff of the $l = s_1$ mode, $c_l/c \to \infty$ such that from Eq. (3a), $\theta_l \to 0$; the SEW radiates nearly backwards directly (along ray B"A" with B and B" shifted closer to C" than in Fig. 1) without having navigated the far side of the sphere. Such radiation is *not included* in the ray representation [5,6] leading to Eq. (1). The difficulties in the ka region between 70 and 80 were not present in a ray representation of the *forward* scattering. Using the optical theorem, the total scattering cross section is well approximated from the synthesized forward amplitude [12].

4. RAY REPRESENTATION FOR SPHERES FROM ANALYSIS FOR CYLINDERS

The connection between Eq. (1) and rays due to the repeated circumnavigation of SEW may be seen as follows [5]. For either the sphere or cylinder case, the ray representation of the f_l is

$$f_l = \sum_{m=0}^{\infty} f_{ml}, \qquad f_{ml} = -G_l \exp(i\eta_l) \exp\left[-2(\pi - \theta_l)\beta_l\right] z^m, \qquad (14,15)$$

$$z = \exp(-2\pi\beta_l) \exp[-i\pi(j + 1)/2] \exp(i2\pi ka\, c/c_l), \qquad (16)$$

where as in Sec. 2, m is the circumnavigation index and the phase factor depending on $j = \pm 1$ accounts for the caustics at the poles of a sphere. Summation of Eq. (15) as a geometrical series yields Eq. (1). While the form in Eq. (1) is useful for describing resonances, Eq. (14) gives a simpler description of the scattering of short tone bursts. Note that $|f_{ml}| = A_{ml}$ ($\gamma = 0$) of Eq. (7).

While the coefficient G_l accounts for the local coupling of the sound field in the fluid with the SEW in the cylinder case, it also includes the effects of axial focusing [2,13] in the sphere case. For the cylinder case, Eq. (2) is replaced by Eq. (17) below:

$$\frac{p_{sca}}{p_{inc}} = \left(\frac{a}{2r}\right)^{1/2} f \exp[i(kr - \omega t)], \qquad |f_{ml}| = 2\sqrt{2}\; |p_{mle}|/|p_{inc}| \qquad (17,18)$$

and Eq. (18), which follows from (17) and consideration of ray tubes, expresses $|f_{ml}|$ in terms of the local pressure amplitude $|p_{mle}|$ of the corresponding outgoing wave in the *exit plane* (Fig. 1)of the *cylinder* from either of two virtual line sources. For cylinders, Eqs. (15) and (18) may be combined to describe the amplitude of the wave diverging from the virtual line source at F_l. (The factor 2 in Eq. (17) accounts for the virtual source, not shown, displaced *above* C by b_l.) The corresponding relationship between $|f_{ml}|$ of a *sphere* and the local amplitude $|p_{mle}|$ in the exit plane is complicated by axial focusing. Approximation of the relevant diffraction integral [13] gives for the sphere case

$$|f_{ml}| \approx \frac{2k|p_{mle}|}{a|p_{inc}|} \left| \int_0^{\infty} s \exp\left[ik\, (s-b_l)^2/2a \right] ds \right| \approx (8\pi ka)^{1/2} \frac{|p_{mle}|}{|p_{inc}|}\left(\frac{b_l}{a} + O(ka)^{-1/2}\right), \qquad (19)$$

where $b_l = ac/c_l$ is the focal circle radius and it is assumed that $ka \gg 1$ and b_l/a is not $\ll 1$. Given Eq. (5) for $|G_l|$ of a cylinder, the $|f_{ml}|$ for the sphere may be approximated as follows. Consider a cylinder having the same β_l, c_l, radius a, and p_{inc} as the sphere of interest. Consideration of the energy flux along ray tubes on the surface of each scatterer gives $|p_{mle}$ (sphere)$|$ $\approx |p_{mle}$ (cylinder)$|$. Hence $|p_{mle}/p_{inc}|$ may be eliminated from the right side of (19) by using Eqs. (18), (15), and (5). The result for the sphere is that $|f_{ml}|$ is as in Eq. (15) with $|G_l|$ given by Eq. (4). Hence G_l of a sphere in Eq. (4) accounts for the effects of axial focusing on the far field amplitude as approximated by Eq. (19) when b_l/a is not $\ll 1$.

Extension of the ray arguments above gives $\arg(G_l^{sp}) \approx \arg(G_l^{cy}) - \pi/4$ when phase information is retained at all stages. Approximations for $\arg(G_l)$ for either case may be obtained by retaining phase information in the comparison of Eq. (1) with a Breit-Wigner form function from RST. (In the latter, a rigid background is assumed to be appropriate [8].) Because of limitations on RST, the

comparison may only be valid if $\beta_l \ll 1$. The results are:

$$\arg(G_l^{sp}) \approx 0, \qquad \arg(G_l^{cy}) \approx \pi/4 \qquad\qquad (20,21)$$

in agreement with the relationship noted above. It is evident from Figs. 3 and 4 that Eqs. (4) and (20) are applicable in the problems considered.

Consider now SEW contributions to the backscattering from a sphere which is only slightly deformed into the shape of a spheroid. The outgoing wavefront is no longer toroidal, but is perturbed. Consequently the axial caustic (which led to the γ dependence of Eq. (7)) is unfolded to give an astroid caustic which has a more complicated directional dependence [14].

ACKNOWLEDGMENTS

REFERENCES

[1]   Keller, J. B., IEEE Trans. Ant. Propag. AP-23 (1985) 123.
[2]   Marston, P. L., Williams, K. L., and Hanson, T. J. B., J. Acoust. Soc. Am. 74 (1983) 605.
[3]   Borovikov, V. A. and Veksler, N. D., Wave Motion 7 (1985) 143.
[4]   Williams, K. L. and Marston, P. L., J. Acoust. Soc. Am. 78 (1985) 1093.
[5]   Williams, K. L. and Marston, P. L., J. Acoust. Soc. Am. 79 (1986) 1702.
[6]   Marston, P. L., J. Acoust. Soc. Am. 83 (1988) 25.
[7]   Williams, K. L. and Marston, P. L., J. Acoust. Soc. Am. 78 (1985) 722.
[8]   Flax, L., Dragonette, L. R., and Uberall H., J. Acoust. Soc. Am. 63 (1978) 723.
[9]   Marston, P. L., J. Acoust. Soc. Am. 85 (1989) 2663.
[10] Kargl, S. G. and Marston, P. L., J. Acoust. Soc. Am. 85 (1989) 1014.
[11] Felsen, L. B., Ho, J. M., and Lu, I. T., J. Acoust. Soc. Am. (to be published).
[12] Marston, P. L. and Kargl, S. G., in: Oceans '89 Conference Record (IEEE, New York, 1989) pp. 1194-1198.
[13] Marston, P. L. and Langley, D. S., J. Acoust. Soc. Am. 73 (1983) 1464.
[14] Arnott, W. P. and Marston, P. L., J. Acoust. Soc. Am. 85 (1989) 1427.

APPENDIX B (For the same Proceedings as Appendix A)

TRANSVERSE CUSP DIFFRACTION CATASTROPHES PRODUCED BY REFLECTING ULTRASONIC TONE BURSTS FROM CURVED SURFACES

Carl K. Frederickson and Philip L. Marston*

Department of Physics
Washington State University
Pullman, Washington 99164

An experiment is summarized in which transverse cusp caustics and associated wavefields are produced by reflecting high-frequency sound and light from smooth curved metal surfaces in water. Structure in the sound field having the form of a Pearcey pattern is clearly observed. It is useful for inverse scattering.

1. INTRODUCTION

Caustics may be classified according to the catastrophe designation of a singularity associated with the merging of rays [1]. The wavefield patterns in regions near caustics are often referred to as "diffraction catastrophes," and while wave amplitude may be large, it does not diverge at caustics as predicted from elementary geometrical optics. The caustic having the generic shape of a cubic cusp curve is associated with the merging of three rays at a cusp point and the disappearance of two rays as the caustic is crossed. The present paper concerns cusp caustics oriented as shown in Fig. 1. The direction of propagation of some outgoing wavefront (produced by reflection in the present study) is nearly parallel to the z axis. The wavefront propagates from the exit plane in water to produce the caustic. The cusp of interest opens up generally transverse to the z axis such that in the uv plane (which is parallel to the exit plane) the caustic coordinates are given by Eq. (1),

$$D_T(u - u_c)^3 = (v - v_c)^2, \qquad D_L(z - z_c)^3 = v^2 \qquad (1,2)$$

where for comparison, Eq. (2) shows the form of an axial (or longitudinal) caustic in the zv plane. The coefficients D_T and D_L are cusp opening rates and (u_c, v_c) and $(z_c, v_c = 0)$ are cusp point coordinates in the transverse and axial cases, respectively. The axial caustic is generally associated with aberration of focused cylindrical wavefronts [2] and near the cusp point the Pearcey function

$$P(w_2, w_1) = \int_{-\infty}^{\infty} \exp\left[i\left(s^4 + w_2 s^2 + w_1 s\right)\right] ds, \qquad (3)$$

describes the wavefield with w_2 and w_1 proportional to $\pm(z - z_c)$ and $\pm v$, respectively [3]. Near a transverse cusp, Marston [4] has shown how the relevant *two-dimensional* diffraction integral reduces to $P(w_2, w_1)$ with w_2 and w_1 proportional to $\pm(u - u_c)$ and $\pm(v - v_c)$, respectively. Plots of $|P(w_2, w_1)|$ display a diffraction structure known as a Pearcey pattern.

A previous study in which an ultrasonic wavefield near a cusp caustic was scanned by Dong *et al.* [5] failed to resolve a Pearcey pattern. Our experiments are based on the prediction that an outgoing wavefront displaced from the xy plane in the form [4, 6, 7]

$$W(x,y) = -(a_1 x^2 + a_2 y^2 x + a_3 y^2 + a_4 x + a_5 y), \qquad a_2 \neq 0, \qquad (4)$$
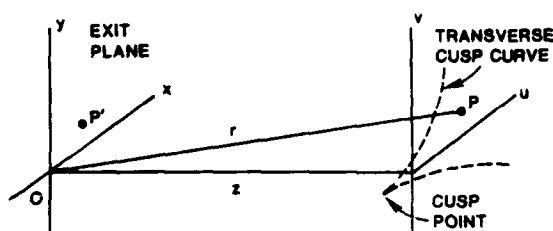
FIGURE 1

Coordinate system for describing a wavefront
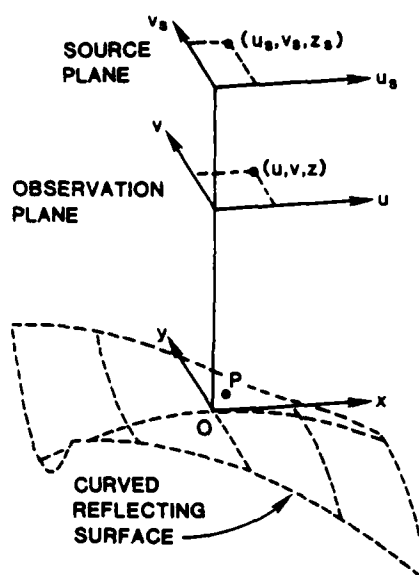near the exit plane and the resulting caustics.

FIGURE 2

(Right) A wave from the point source reflects
to produce a cusp diffraction catastrophe in the
observation plane. The surface has $c_2 < 0$.

propagates to produce a transverse cusp in the plane at z provided $a_1 \neq - (2z)^{-1}$. The relation
between the shape parameters a_i and the caustic parameters $D_T(z)$ and (u_c, v_c) is known in the
paraxial approximation [4]. Marston [6] calculated that a reflected wavefront having the shape of
Eq. (4) is produced by reflecting sound from a point source off of a surface whose height is

$$h(x,y) = c_1 x^2 + c_2 y^2 x + c_3 y^2 + c_4 x + c_5 y, \quad c_2 = -a_y/2 \neq 0, \tag{5}$$

relative to the xy plane with $a_1 = -2c_1 + (2z_s)^{-1} \neq -(2z)^{-1}$ where (u_s, v_s, z_s) denote source point
coordinates as shown in Fig. 2. The relationship between the shape parameters c_i, the source
location and the wavenumber $2\pi/\lambda = 2\pi f/c$ with the w_1 and w_2 of the Pearcey pattern and the
caustic parameters are calculated in Ref. 6 in the paraxial approximation.

Wavefield data should be useful for inferring the local shape of the reflector which produces the
caustic [6]. In related research, optical diffraction catastrophes in scattering from oblate water
drops were discovered [8]. Relationships between a scatterer's aspect ratio, wavefront shape,
caustic parameters, and diffraction catastrophe patterns have been derived [7, 9-11].

2. SUMMARY OF EXPERIMENTAL METHOD AND RESULTS

A transducer was situated in water which simulated a point source at $z_s = 141$ cm. The duration τ
of the tone burst radiated by the transducer was sufficiently long ($\tau \geq 400$ µs) that all of the echoes
from the curved surface overlapped in the region of time and space imaged in the reflected field by
raster scanning a small hydrophone receiver in the uv observation plane. The duration τ was
sufficiently short that the reflected wave could be sampled distinct from the incident wave. The
hydrophone voltage was amplified and rectified and then gated and sampled at an appropriate time
to simulate a stead-state reflection. The resulting voltage was stored on a Mac II computer along
with the current hydrophone position. This was repeated for a large number of positions in the
scan. An image was produced by increasing the pixel brightness on a display with the aforemen-
tioned voltage for a pixel position corresponding to each hydrophone position. Figure 3 is a repre-
sentative photograph of the display which clearly shows the Pearcey pattern of a transverse cusp
diffraction catastrophe. Dark regions correspond to regions of low reflected pressure amplitude.

One approach to testing the theory would require accurate direct measurements of c_1 and c_2 in
Eq. (5). We chose a different method based on comparison with the optical cusp caustic produced
by placing an optical point source at the same location as the acoustic source. This was done with
the aid of an optical fiber (driven by a laser) with its output end in the water tank. The receiver was
replaced by a photo detector. The output voltage was stored and imaged as described above.
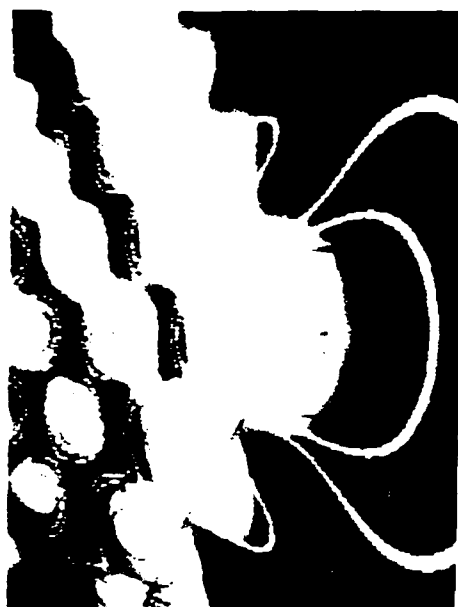
FIGURE 3

FIGURE 4

Measured ultrasonic wavefield pattern with $z =$ 68 cm and $f = 1.0$ MHz. The displayed spread in u and v are 8.0 and 10.8 cm, respectively.

Measured pattern of reflected light. Superposed is a faint cusp curve having $D_T = 1.38$/cm which is used in the theoretical contours in Fig. 3.

Figure 4 shows the resulting image of the optical caustic with the same reflecting surface, source location, and observation plane as in Fig. 3 but with λ smaller by a factor > 3000. Superposed on Fig. 4 is a cusp curve given by Eq. (1) in which D_T and the cusp point location (u_c, v_c) were empirically fitted. A cusp curve with the same D_T is superposed on Fig. 3 since from the theory [6] the acoustical D_T is the same. Also shown in Fig. 3 are theoretical contours of constant $P(w_2, w_1)$ in which the only remaining free parameter a_1 was varied for agreement between the patterns. From the fitted a_1 and D_T, the surface parameters c_1 and c_2 were inferred and were near the range determined by direct measurement for the surface. The cusp is oriented as predicted. Patterns similar to Fig. 3 were observed for f from 0.5 to 4 MHz where along the u axis the spacing scales as $f^{-1/2}$. The observations not only verify the existence of the transverse Pearcey pattern but support its use in the inverse problem of determining the local surface shape.

REFERENCES

[1]   Berry, M. V. and Upstill, C., Progress in Optics 18 (1980) 257.
[2]   Solimeno, S., Crosignani, B., and DiPorto, P., Guiding, Diffraction, and Confinement of Optical Radiation (Academic, Orlando, 1986).
[3]   Pearcey, T., Philos. Mag. 37 (1946) 311.
[4]   Marston, P. L., J. Acoust. Soc. Am. 81 (1987) 226; 83 (1988) 1976.
[5]   Dong, R., Adler, L., and Doyle, P. A., J. Appl. Phys. 54 (1983) 2832.
[6]   Marston, P. L., Surface Shapes Giving Transverse Cusp Catastrophes in Acoustic or Seismic Echoes, in: Kessler, L. W. (ed.), Acoustical Imaging Vol. 16 (Plenum, New York, 1988) pp 579-588.
[7]   Marston, P. L. in: Schmidt, S. C. and Holmes, N. C. (eds.) Shock Waves in Condensed Matter 1987 (North-Holland, Amsterdam, 1988) pp. 203-206.
[8]   Marston, P. L. and Trinh, E. H., Nature 312 (1984) 529.
[9]   Marston, P. L., Optics Letters 10 (1985) 588.
[10]   Marston, P. L., Dean, C. E., and Simpson, H. J., in: Wang, T. G. (ed. Proceedings of the Third International Colloquium on Drops and Bubbles (AIP Conf. Proceedings, N. Y., 1989)
[11]   Arnott, W. P. and Marston, P. L., J. Acoust. Soc. Am. 85 (1989) 1422.

OFFICE OF NAVAL RESEARCH

PUBLICATIONS / PATENTS / PRESENTATIONS / HONORS REPORT

FOR

1 OCTOBER 19 __88__ through 30 SEPTEMBER 19 __89__

****

CONTRACT N00014 - __85-C-0141__

R&T NO. __4126934__

TITLE OF CONTRACT: __Propagation and Effects of Acoustical and Optical Waves__

NAME(S) OF PRINCIPAL INVESTIGATOR(S) __Philip L. Marston__

NAME OF ORGANIZATION: __Washington State University__

ADDRESS OF ORGANIZATION: Department of Physics, Washington State University
Pullman, WA 99164-2814

****

PAPERS SUBMITTED TO REFEREED JOURNALS
(Not yet published)

1. S. G. Kargl and P. L. Marston, "GTD synthesis of Lamb wave contributions to the total scattering cross section for an elastic spherical shell," *Journal of the Acoustical Society of America* (submitted July, 1989).

PAPERS PUBLISHED IN REFEREED JOURNALS

1. S. G. Kargl and P. L. Marston, "Observations and modeling of the backscattering of short tone bursts from a spherical shell: Lamb wave echoes, glory, and axial reverberations," *Journal of the Acoustical Society of America* **85**, 1014-1028 (1989).

2. W. P. Arnott and P. L. Marston, "Unfolding axial caustics of glory scattering with harmonic angular perturbations of toroidal wavefronts," *Journal of the Acoustical Society of America* **85**, 1427-1440 (1989).

3. P. L. Marston, "Phase velocity of Lamb waves on a spherical shell: Approximate dependence on curvature from kinematics, *Journal of the Acoustical Society of America* **85**, 2663-2665 (1989).

PAPERS PUBLISHED IN NON-REFEREED JOURNALS

1. P. L. Marston, "Light Scattering from Bubbles in Water," *Oceans' 89 Proceedings* (IEEE, New York, 1989) pp. 1186-1193; research partially supported by the Naval Ocean Research and Development Activity.

2. P. L. Marston and S. G. Kargl, "Elastic Surface Wave Contributions to Backscattering from Smooth Objects Described by a Generalization of GTD," *Oceans' 89 Proceedings* (IEEE, New York, 1989) pp. 1194-1198.

TECHNICAL REPORTS PUBLISHED

1. P. L. Marston, *Research on Acoustical Scattering, Diffraction Catastrophes, Optics of Bubbles, and Acoustical Phase Conjugation*, Annual Summary Report, issued October 1988 (Defense Technical Information Center, Alexandria, VA, Accession No. AD-A2011451) 52 pages.

Note: In the "Publications, Patents, ... Report" for 1988 the following item was listed without the DTIC Accession Number. It is relisted here since that information is now known:

S. M. Bäumer, *Observation of Brewster angle light scattering from air bubbles rising in water* (M.S. thesis, Washington State University, 1988), issued as a Technical Report, September 1988 (Defense Technical Information Center, Alexandria, VA, Accession No. AD-A199582) 104 pages.

BOOKS (AND SECTIONS THEREOF) SUBMITTED FOR PUBLICATION

N/A

BOOKS (AND SECTIONS THEREOF) PUBLISHED

P. L. Marston and D. S. Langley, "Bubbles in Liquid ^{4}He and ^{3}He: Mie and Physical-Optics Models of Light Scattering, and Quantum Tunneling and Spinodal Models of Nucleation," in *Near Zero: New Frontiers in Physics*, edited by J. D. Fairbank, B. S. Deaver, C. W. F. Everitt, and P. F. Michelson (Freeman, San Francisco, 1988) pp. 127-140; research partially supported by an Alfred P. Sloan Research Fellowship held by P. L. Marston at the time of the work.

PATENTS FILED

N/A

PATENTS GRANTED

N/A

INVITED PRESENTATIONS AT TOPICAL OR SCIENTIFIC/TECHNICAL SOCIETY CONFERENCES

1. P. L. Marston, "Elastic Resonance Amplitudes Described by: Generalized GTD and Product Expansion of the S Function," at the *Symposium on Acoustic Resonance Scattering* (Catholic University, Washington, D.C., May 1989).

2. P. L. Marston, S. G. Kargl, and K. L. Williams, "Rayleigh, Lamb, and Whispering Gallery Wave Contributions to Backscattering from Smooth Elastic Objects in Water Described by a Generalization of GTD," at the *IUTAM Symposium on Elastic Wave Propagation and Ultrasonic Nondestructive Evaluation*, Boulder, CO, July/Aug. 1989).

HONORS/AWARDS/PRIZES

P. L. Marston, Fellow Membership Status, Acoustical Society of America, December, 1988.

GRADUATE STUDENTS SUPPORTED UNDER
CONTRACT FOR YEAR ENDING 30 SEPTEMBER 1989

1. Cleon E. Dean (Ph.D. Physics, August 1989).

2. Carl K. Frederickson (Ph.D. Candidate)

3. Steven G. Kargl (Ph.D. Candidate)

4. Harry J. Simpson (Ph.D. Candidate)

5. J. Michael Winey (M.S. Candidate)

6. Jeff R. Filler (Ph.D. Candidate, Engineering)

POSTDOCTORAL SUPPORTED UNDER
CONTRACT FOR YEAR ENDING 30 SEPTEMBER 1989

1. Cleon E. Dean (Partially supported since August 15, 1989).

CONTRIBUTED PRESENTATIONS AT
TOPICAL OR SCIENTIFIC/TECHNICAL CONFERENCES

1. P. L. Marston, "Product expansion of the S function for scattering from elastic spheres having multiple resonances," [J. Acoust. Soc. Am. Suppl. **84**, 185 (1988)] *2nd Joint Meeting of the Acoustical Societies of Japan and America* (Honolulu, November 1988).

2. S. G. Kargl and P. L. Marston, "Forward-glory scattering from a spherical shell and backscattering from a convex hemispherical shell," J. Acoust. Soc. Am. Suppl. **84**, S208 (1988), *2nd Joint Meeting of the Acoustical Societies of Japan and America* (Honolulu, November 1988).

3. S. G. Kargl and P. L. Marston, "Total scattering cross section of an elastic spherical shell: Comparison of exact computations with a GTD model that includes Lamb wave resonances," [J. Acoust. Soc. Am. Suppl. **85**, 95 (1989)], *Acoustical Society of America* (Syracuse, NY, May 1989).

4. S. G. Kargl and P. L. Marston, "GTD synthesis of resonance amplitudes in the backscattering from an elastic spherical shell," [J. Acoust. Soc. Am. Suppl. **85**, 150 (1989)], *Acoustical Society of America* (Syracuse, NY, May 1989).

5. C. K. Frederickson and P. L. Marston, "Transverse Pearcey patterns observed in the reflection of ultrasound from curved surfaces," [J. Acoust. Soc. Am. Suppl. **85**, 150 (1989)], *Acoustical Society of America* (Syracuse, NY, May 1989).*Acoustical Society of America* (Syracuse, NY, May 1989).

6. P. L. Marston and C. K. Frederickson, "Transverse Cusp Diffraction Catastrophes Produced by Reflecting Ultrasonic Tone Bursts from Curved Surfaces in Water and Other Novel Caustics," Poster Presentation at the *IUTAM Symposium on Elastic Wave Propagation and Ultrasonic Nondestructive Evaluation* (Boulder, CO, July/Aug. 1989).

7. J. R. Filler and W. C. Mih, "Shear Layer Vortices Separating from a Cylinder at Low Reynolds Numbers," Poster Presentation at the *Seventh Symposium on Turbulent Shear Flows* (Stanford University, Palo Alto, CA, Aug. 1989); research partially supported by Washington State University Albrook Hydraulics Lab.

8. P. L. Marston, "Light Scattering from Bubbles in Water," Oceans' 89, Oceanic Engineering Society of the IEEE (Seattle, WA, Sept. 1989); research partially supported by the Naval Ocean Research and Development Activity.

9. P. L. Marston and S. G. Kargl, "Elastic Surface Wave Contributions to Backscattering from Smooth Objects Described by a Generalization of GTD," Oceans' 89, Oceanic Engineering Society of the IEEE (Seattle, WA, Sept. 1989).

REPORTS DISTRIBUTION FOR ONE PHYSICS DIVISION, UNCLASSIFIED CONTRACTS

Director
Defense Advanced Research Projects Agency
1400 Wilson Blvd.
Arlington, VA 22209-2308
1 copy

Lawrence Livermore Laboratory
Attn: Dr. W. F. Krupke
P.O. 808
Livermore, CA 94550
1 copy

Naval Avionics Facility
Technical Library
Indianapolis, IN 46218
1 copy

Professor Julian Maynard
Department of Physics
Pennsylvania State University
University Park, PA 16802

Office of Naval Research
Physics Division Office (Code 1112)
800 North Quincy Street
Arlington, VA 22217-5000

Harry Diamond Laboratories
Technical Library
2800 Powder Mill Road
Adelphi, MD 20783
2 copies

Naval Ocean Systems Center
Technical Library
San Diego, CA 92152
1 copy

Professor Wolfgang Sachse
Theoretical and Applied Mechanics
Cornell University
Ithaca, NY 14853-1503

Office of Naval Research
Director, Technology (Code 20)
800 North Quincy Street
Arlington, VA 22217-5000
1 copy

Naval Weapons Center
Technical Library (Code 753)
China Lake, CA 93555
1 copy

SUPPLEMENTAL DISTRIBUTION (1 copy each)

Professor James Wagner
Materials Science and Engineering
The Johns Hopkins University
Baltimore, MD 21218

Naval Research Laboratory
Department of the Navy (Code 2625)
Washington, D.C. 20375-5000
1 copy

Naval Underwater Systems Center
Technical Center
New London, CT 06320
1 copy

Professor Henry Bass
Department of Physics and Astronomy
University of Mississippi
University, MS 38677
1 copy

Professor Robert Apfel
Yale University
P.O. Box 2159
New Haven, CT 06520

Office of the Director of Defense
Research and Engineering
The Pentagon, Rm. 3E1006
Washington, D.C. 20301
1 copy

Commandant of the Marine Corps
Scientific Advisor (Code RD-1)
Washington, D.C. 20380
1 copy

Dr. David Blackstock
Applied Research Laboratories
University of Texas
P.O. Box 8029
Austin, TX 78713-8029
1 copy

Dr. Roger Hackman
Code 4120
Naval Coastal Systems Center
Panama City, FL 32407-5000

U.S. Army Research Office
Box 1211
Research Triangle Park
North Carolina 27709-2211
1 copy

Naval Ordnance Station
Technical Library
Indian Head, MD 20640
2 copies

Mr. Franklin Rschmidge
National Bureau of Standards
Gaithersburg, MD 20899
1 copy

Dr. W. P. Arnott
National Center for Physical Acoustics
P.O. Box 847
University, MS 38677

Defense Technical Information Center
Cameron Station
Alexandria, VA 22314
2 copies

Naval Postgraduate School
Technical Library (Code 0212)
Monterey, CA 93940
2 copies

Professor Lawrence Crum
National Center for Physical Acoustics
P.O. Box 847
University, MS 38677
1 copy

Dr. Kevin Williams
Applied Physics Laboratory
University of Washington
Seattle, WA 98195

Director
National Bureau of Standards
Attn: Technical Library (Admin B-01)
Gaithersburg, MD 20899
1 copy

Naval Missile Center
Technical Library (Code 5632.2)
Point Mugu, CA 93010
1 copy

Professor Steven Garrett
Department of Physics - Code 61Gx
Naval Postgraduate School
Monterey, CA 93943-5000
1 copy

Professor Calvin Quate
Department of Applied Physics
Stanford University
Stanford, CA 94305

Commander
U.S. Army
Attn: Technical Library (STINFO-ET)
Fort Belvoir, VA 22060-5605
1 copy

Naval Ordnance Station
Technical Library
Louisville, KY 40214
1 copy

Professor Robert Green
Materials Science and Engineering
The Johns Hopkins University
Baltimore, MD 21218
1 copy

Professor Andrew Atchley
Department of Physics - Code 61AY
Naval Postgraduate School
Monterey, CA 93943-5000

ODDR&E Advisory Group on Electron Devices
201 Varick Street, 11th Floor
New York, NY 10014-4877
1 copy

Commanding Officer
Naval Ocean Research & Development Activity
NSTL Station, MS 39529
1 copy

Professor Mark Hamilton
Department of Mechanical Engineering
University of Texas
Austin, TX 78712-1063
1 copy

Prof. L. B. Felsen
Dept. of Electrical Engineering
Polytechnic Institute of New York
Room 110
Farmingdale, NY 11570

Air Force Office of Scientific Research
Department of the Air Force
Bolling AFB, D.C. 22209
1 copy

Naval Surface Weapons Center
Technical Library
Silver Spring, MD 20910
1 copy

Professor Mahlon Levy
Department of Physics
The University of Wisconsin-Milwaukee
Milwaukee, WI 53201
1 copy

Dr. Robert N. Thurston
Bell Communications Research
Guided Wave and Optoelectronics
331 Newman Springs Road
Red Bank, NJ 07701

Air Force Weapons Laboratory
Technical Library
Kirtland Air Force Base
Albuquerque, NM 87117
1 copy

Naval Ship Research & Development Center
Central Library (Codes L42 and L43)
Bethesda, MD 20084
1 copy

Professor Walter Mayer
Department of Physics
Georgetown University
Washington, D.C. 20057
1 copy